MOANMORE LOWER WIND FARM:
COLLISION RISK MODELLING REPORT

Tom Gittings BSc, PhD, MCIEEM
Ecological Consultant
3 Coastguard Cottages
Roches Point
Whitegate
CO. CORK
www.gittings.ie

REPORT NUMBER: 2408-F1
STATUS OF REPORT: Revision 2
DATE OF REPORT: 14 November 2024

CONTENTS

LIST OF FIGURES

LIST OF MAPS

SUMMARY

This report presents the results of collision risk modelling for the proposed Moanmore Lower Wind Farm, Co. Clare. The wind farm will comprise three turbines. The turbines will have a hub height of 82 m and a rotor diameter of 136 m, which creates a potential collision height airspace of 14-150 m.

The collision risk model was based on seven seasons of vantage point survey data from one vantage point, and three seasons from a second vantage point, with a survey effort of six hours / month / vantage point. The SNH / Band model was used, with the VP averaging method used for the stage 1 model.

The predicted collision risk for Kestrel would result in 44 collisions over the 30-year lifespan of the wind farm. However, there may have been some approximations in the recording of Kestrel flight activity that resulted in overestimation of the predicted collision risk (see Section 6.2 and 6.3.4).

The predicted collision risks would also result in at least one collision over the 30-year lifespan of the wind farm for Grey Heron, Hen Harrier, Buzzard and Whimbrel. However, the Hen Harrier collision risk was probably overestimated due to the mismatch between the height bands used for the vantage point survey and the ground clearance of the proposed turbine.

The use of 1 km viewsheds substantially reduced the potential effects of under-detection of distant flightlines on the collision risk predictions. Correction factors were also included in the model to further address these effects.

To allow for the uncertainty associated with sampling effects, the predicted collision risks should be multiplied by factors of around 2-3 to represent a worst case scenario of the sampled flight activity being at the lower limit of the theoretical confidence intervals of the distribution of samples from the complete flight activity dataset. However, for Kestrel, the potential overestimation of the collision risk due to inclusion of hovering flight activity in the standard stage 1 model should also be considered.

1. INTRODUCTION

1.1. SCOPE

This report presents the results of collision risk modelling for the proposed Moanmore Lower Wind Farm, Co. Clare. The proposed wind farm will comprise three turbines. The site location and proposed site layout is shown in Map 1.1. The turbines will have a hub height of 82 m and a rotor diameter of 136 m, which creates a potential collision height airspace of 14-150 m.

This work was commissioned by Greensource. The collision risk modelling and reporting was carried out by Tom Gittings.

1.2. COLLISION RISK MODELLING

Collision risk modelling uses statistical modelling techniques to predict the likely collision risk. It uses flight activity data from before the construction of a wind farm to calculate the likely risk of birds colliding with turbines in the operational wind farm. There are three stages to the collision risk model. In stage 1, the flight activity data that was recorded is scaled up to represent the overall level of flight activity in the wind farm site across the relevant period (e.g., a full year for a resident species, or a summer or winter for a migrant species). The number of predicted transits of the rotor swept volume in the wind farm is then calculated based on the proportion of the total air space that is occupied by the rotor swept volume. However, most transits of the rotor swept volume will not result in a collision, because for the duration of a transit, most of the rotor swept volume is not occupied by the turbine blades. Therefore, stage 2 of the collision risk model involves calculating the probability that a bird will collide with a turbine blade when it transits the rotor swept volume. Most birds try to avoid the turbine blades, either by avoiding the wind farm area altogether, or by taking evasive action if they are likely to collide with a blade while transiting the wind farm, so it is also necessary to factor in an avoidance rate. This is done in the final stage, where the predicted number of transits are converted to predicted number of collisions by multiplying by the collision probability (assuming no avoidance behaviour) and then correcting for the avoidance rate and other relevant factors.

1.3. STATEMENT OF COMPETENCE

Tom Gittings has a BSc in Ecology, a PhD in Zoology and is a member of the Chartered Institute of Ecology and Environmental Management. He has 28 years' experience in professional ecological consultancy work and research. He has specific expertise in ornithological assessments for wind energy projects and has been involved in numerous wind energy projects. His input to these projects has variously included field surveys (including vantage point surveys, breeding wader and raptor surveys and wintering waterbird surveys), collision risk modelling, writing the ornithological sections of EIS/EIAR and NIS reports, expert witness services at oral hearings, and provision of scoping advice and peer review services.

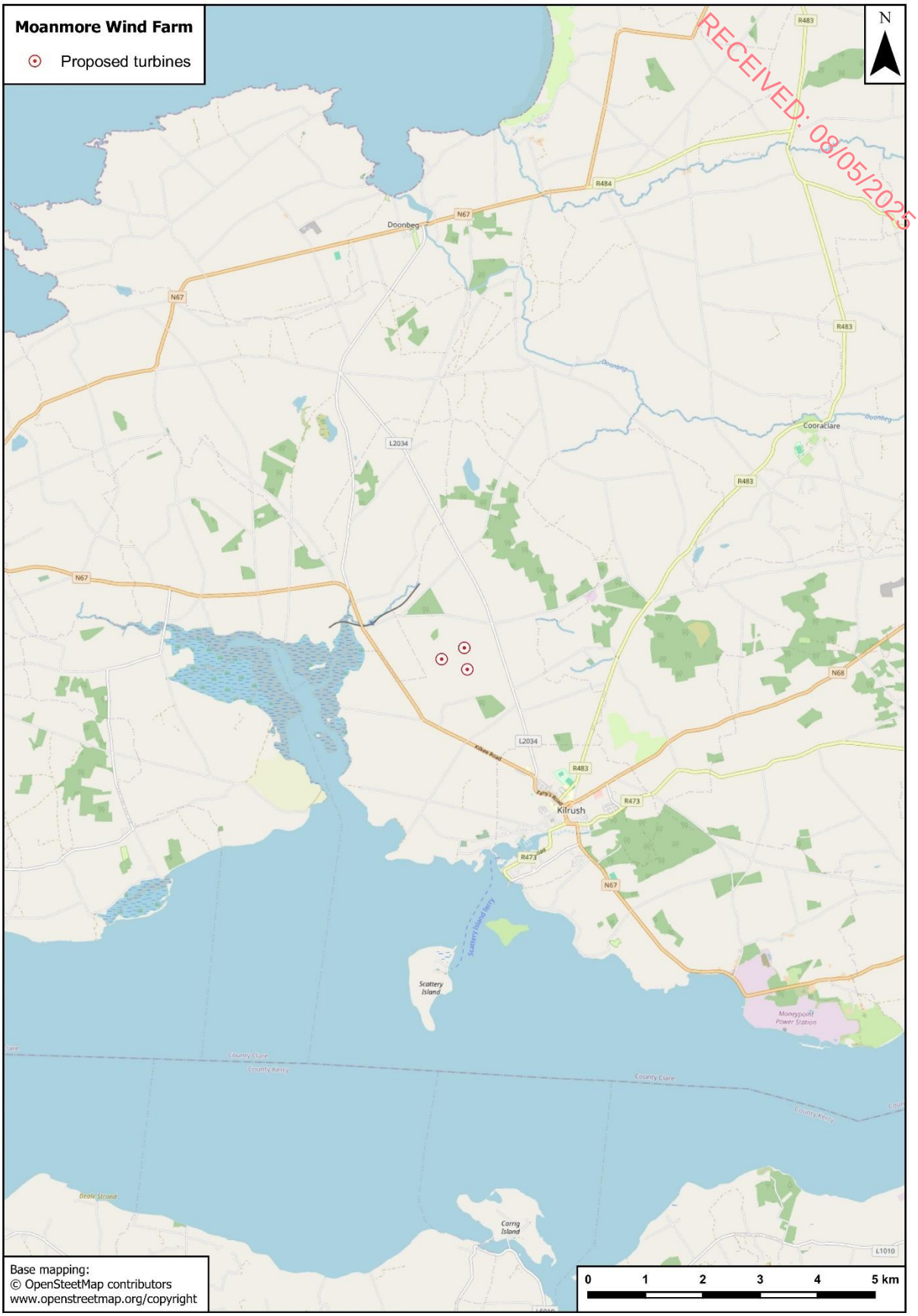

Map 1.1. Site location.

2. METHODS

2.1. GENERAL APPROACH

The collision risk modelling methodology was based on the SNH guidance on collision risk modelling (SNH, 2000), and current practice in collision risk modelling.

2.2. DATA SOURCES

The flight activity data used for the collision risk model comprised a vantage point survey that was carried out over seven seasons between October 2020 and March 2024.

The vantage point locations and the viewshed arcs used for the vantage point survey are shown in Map 2.1.

One vantage point (VP1) was surveyed monthly from October 2020 to March 2024, while a second vantage point (VP2) was surveyed monthly from October 2022 to March 2024. Six hours of vantage point watches were completed at each vantage point in each month surveyed, amounting to totals of 252 hours at VP1 and 108 hours at VP2 across the survey period.

The survey recorded timed flight activity of raptors and waterbirds in five height bands: 0-20 m, 20-50 m, 50-100 m, 100-180 m, and above 180 m.

The full vantage point survey data is included in Appendix 6.4.

The turbine specifications used for the collision risk model (apart from mean pitch angle; see Section 5.1) were supplied by Greensource and are shown in Table 2.1.

The bird biometric parameters used for the collision risk model are shown in Table 2.2.

Table 2.1. Turbine parameters used for the collision risk model.

Parameter	Value
Hub height	82 m
Rotor diameter	136 m
Max_chord	4.1 m
Rotor speed range	5.6-14.0 m/sec
Midpoint of rotor speed range	9.8 m/sec
Mean pitch angle	0°

Sources: data supplied by Greensource, except for mean pitch for which see Section 5.1.

Table 2.2. Bird biometric parameters used for the collision risk model.

Species	Length (m)	Wingspan (m)	Flight speed (m/sec)
Mallard	0.58	0.9	18.5
Cormorant	0.9	1.45	15.2
Little Egret	0.6	0.915	10.2
Grey Heron	0.94	1.85	11.2
Hen Harrier	0.48	1.1	9.1
Sparrowhawk	0.33	0.62	11.3
Buzzard	0.54	1.2	11.6
Golden Plover	0.28	0.72	17.9
Lapwing	0.295	0.845	12.8
Whimbrel	0.41	0.82	16.3
Curlew	0.55	0.9	16.3
Greenshank	0.315	0.69	12.3
Black-headed Gull	0.36	1.05	11.9
Common Gull	0.41	1.2	13.4
Lesser Black-backed Gull	0.58	1.42	13.1
Herring Gull	0.60	1.44	12.8
Great Black-backed Gull	0.71	1.58	13.7
Kestrel	0.34	0.76	10.1
Merlin	0.28	0.56	10.1
Peregrine	0.42	1.02	12.1

Sources: length and wingspan from Cramp *et al.* (2004); flight speed from Alerstam *et al.* (2007) with the Grey Plover value used for Golden Plover.

2.3. SITE VISIT

I carried out a site visit on 12th July 2024. During this visit, I ground-truthed the viewshed coverage from each vantage point.

2.4. DATA MANAGEMENT

Before beginning the analyses, I audited the flight activity data for data entry errors and missing data.

2.5. REVIEW OF THE VANTAGE POINT SURVEY COVERAGE AND RESULTS

Before beginning the development of the collision risk model, I carried out a review of the vantage point survey coverage and results. This helped to assess the degree of spatial and temporal variability in the recorded flight activity, which needed to be considered in the development of the collision risk model. The results of this review are presented in Section 3.

2.6. COLLISION RISK MODELLING METHODOLOGY

The collision risk modelling methodology is described in Sections 4 - 6 of this report as part of a step-by-step account of the development of the collision risk model.

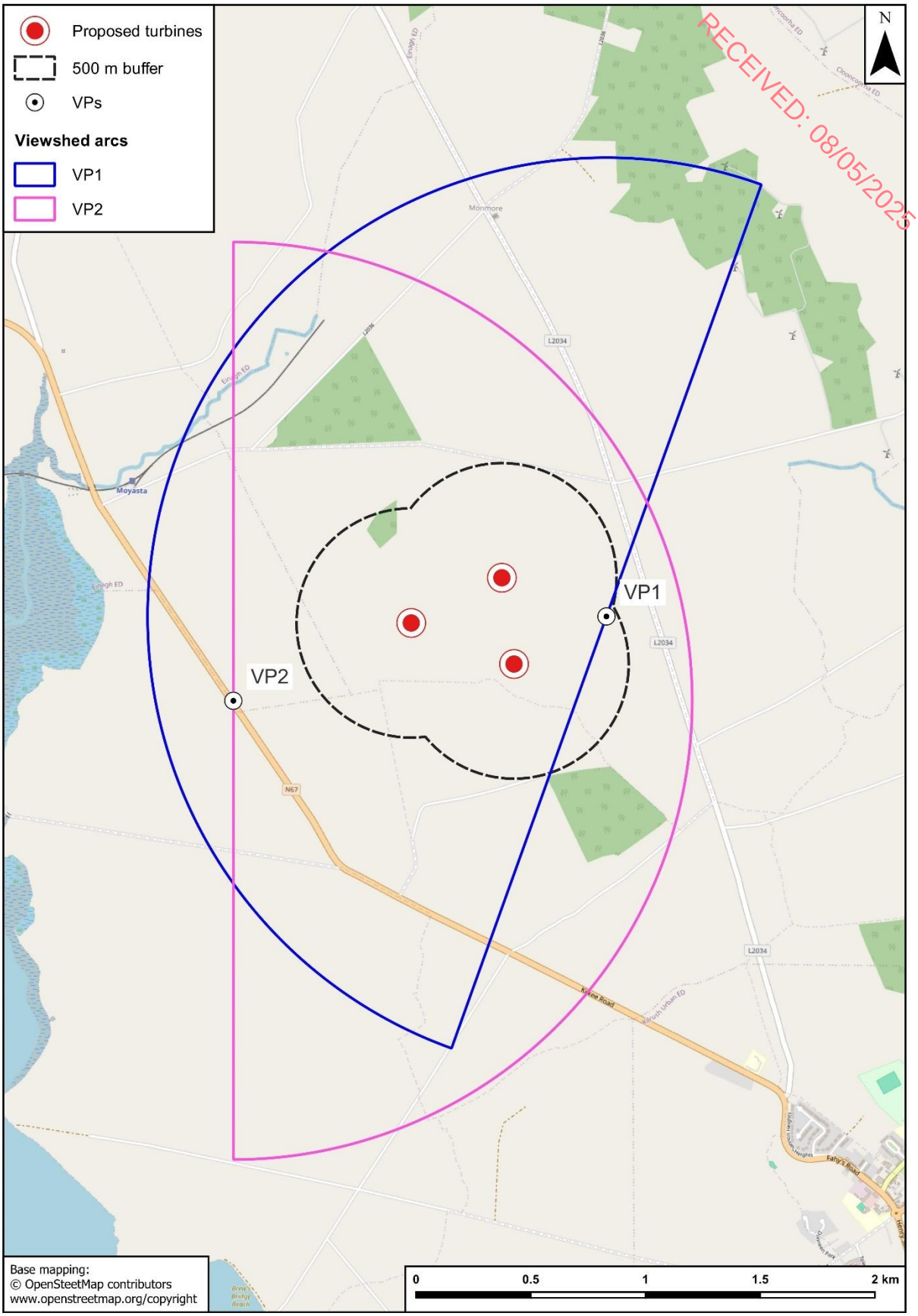

Map 2.1. Vantage points and viewshed arcs used for the vantage point survey.

3. REVIEW OF THE VANTAGE POINT SURVEY COVERAGE AND RESULTS

3.1. EFFECTS OF WEATHER

In the vantage point survey dataset, there were seven watches where the visibility was classified as poor (0.5-1 km) and another 20 watches where the visibility was classified as moderate (1-2 km). These comprised around 23% of the vantage point survey hours completed across all watches. All the other watches had good visibility (> 2 km).

The effect of reduced visibility will be to cause under-detection of flightlines in the more distant parts of the viewsheds. The adjusted viewshed areas that I used in this model provide corrections for under-detection effects (see Section 3.1.1).

3.2. SPATIAL COVERAGE AND VIEWSHEDS

3.2.1. Viewshed arcs

The viewshed arcs for both vantage points include all of the proposed turbine locations and most (VP1), or all (VP2) of the 500 m buffers around those locations (Map 2.1).

On my site visit, I observed that there was good visibility from VP1, but there appeared to be some limitations to the visibility in the southern half of the VP2 viewshed arc.

The landscape within the viewshed arcs comprises open grassland with scattered patches of forestry. The topography is generally level with a low rise around VP1.

3.2.2. Viewshed analyses

I mapped the viewsheds at heights of 14 m, 20 m, 50 m and 100 m above ground level. These represent the ground clearance of the proposed turbines (14 m), and the divisions between the height bands used for the vantage point survey.

I used the shapefile of the vantage point locations and viewshed arcs supplied by.

I used Bluesky Digital Surface Model (DSM) and Digital Terrain Model (DTM) mapping. The DSM mapping was acquired on 31/05/2023, while the DTM mapping was acquired on 15/04/2020. I used the viewshed function from the terra package (Hijamans, 2023) in R version 4.3.2 (R Core Team, 2023) to carry out the analysis.

The viewsheds needed to be mapped with reference to the ground level, as defined by the DTM mapping, but had to take account of vegetation and structures interfering with the viewing lines, as defined by the DSM mapping. Therefore, I mapped a series of viewsheds at 1 m intervals from 0 m to the viewshed height above the DSM mapping. For each pixel, I then selected the viewshed that represented the difference between the target viewshed height and the elevation of the DSM mapping above the DTM mapping: e.g., if the DSM mapping was 10 m higher than the DTM mapping, then the viewshed at 15 m above the DSM mapping represented the viewshed at 25 m above the DTM mapping. I implemented this procedure using a custom script in R.

The outputs of the viewshed mapping procedure were raster maps showing the visibility at the specified height above ground level at a resolution of 1 m^2. This resulted in very complex boundaries to the viewsheds. To simplify the viewshed mapping, I first converted the viewsheds to vector maps. I then simplified the vector maps using the st_simplify function in the sf package (Pebesma, 2018; Pebesma and Bivand, 2023) in R, with a dTolerance value of 25. I also removed small outlying polygons with areas of less than 1 ha.

3.2.3. Viewshed coverage

The viewshed coverage from VP1 was very good with only a few small peripheral areas not covered at 14 m and 50 m and complete coverage of the viewshed arc at 50 m and 100 m (Map 3.1 – Map 3.4).

The viewshed coverage from VP2 was more limited with large gaps in the southern half of the viewshed arc at 14 m and 20 m, while the southernmost section of the arc remained not covered 50 m and 100 m (Map 3.1 – Map 3.4).

3.1. SPATIAL PATTERNS OF FLIGHT ACTIVITY

3.1.1. Distance effects

Analyses of flightline densities

The distribution of the mapped flightlines in relation to the viewshed arcs (Map 3.5) shows that, while there was good viewshed coverage up to the maximum distances of 2 km from the vantage point locations (particularly for VP1), most of the recorded flight activity was concentrated within around 1000 m of the vantage points.

The concentration of mapped flightlines close to the vantage points is a common feature of vantage point surveys and reflects the effects of distance from vantage point locations on the detection of flight activity. A meta-analysis of vantage point survey data from eight Irish wind farm projects found that detection rates of flight activity showed strong decreases at distances of over 1 km from the vantage point locations, and that this under-detection effect causes underestimation of collision risk by factors of around 1.5 to 5 times (Gittings, 2023).

I analysed the distribution of flightlines in 250 m distance bands from each vantage point. I used the 20 m viewsheds and only included flightlines that included some flight activity in the height bands above 20 m. There were strong declines in flightline densities with increasing distance from the vantage point at VP1 (Figure 3.1). At VP2, flightline densities were more evenly distributed up the 500-750 m distance band but then also showed strong declines with increasing distance (Figure 3.1).

I then calculated the weighted mean flightline densities for each distance band across the two viewsheds using Equation 1. This equation standardises the flightline density in each distance band by the total amount of flight activity recorded at that vantage point, to avoid the analyses being biased by vantage points where large amounts of flight activity were recorded.

Equation 1: $FD_{i*} = : (FD_i / FD_{VP}) \times FD_{mean}$

FD_{i*} = weighted flightline density in band i; FD_i = raw flightline density in band i; FD_{VP} = summed flightline densities across all bands in the viewshed containing band i; FD_{mean} = mean of FD_{VP} = across all the vantage points included in the analysis.

The weighted mean flightline densities across the two vantage points showed a consistent decline with distance from the vantage point (Figure 3.2).

These analyses indicate that there were high levels of under-detection of distant flightlines, particularly at distance of more than 1 km from the vantage point locations.

Viewshed distance

The viewshed arcs used for the vantage point survey covered a distance of 2 km from the vantage point locations, which is the maximum distance allowed by the Scottish Natural Heritage guidance. However, the analyses of flightline densities indicate that the effective viewshed coverage was largely limited to areas within 1000 m of the vantage points. Therefore, I used 1 km viewsheds for the collision risk modelling.

The distribution of the mapped flightlines also indicated that the L2034 was used as a boundary to the survey area for VP1, and the N67 was used as a boundary to the survey area for VP2. Therefore, I clipped the VP1 viewshed to exclude areas east of the L2034 and clipped the VP2 viewshed to exclude areas west of the N67.

The viewsheds used for the collision risk modelling are the 1 km clipped viewsheds shown in Map 3.1 – Map 3.4.

Adjusted viewshed areas

The use of 1 km viewsheds for the collision risk modelling substantially reduced the potential effects of under-detection of distant flightlines on the predicted collision risks. However, even within 1000 m of the vantage points, there was still a lesser, but not trivial, potential under-detection effect.

If the pattern of flightline densities is considered to reflect detectability effects, these densities can be used to calculate adjusted viewshed areas that correct for these detectability effects. I calculated adjusted viewshed areas for the 1 km viewsheds used in the collision risk modelling using the formula shown in Equation 2.

Equation 2: $A_{vis*} = sum_{i=1-4}(A_{vis(i)} \times weight_i)$

A_{vis*} = adjusted viewshed area; i = distance band number from 0-250 m (distance band 1) to 750-1000 m (distance band 4); $weight_i$ = mean density in distance band i relative to the highest distance band density.

The adjusted viewshed areas, compared to the original viewshed areas, are shown in Table 3.1. This table also shows correction factors that represent the increase in collision risk generated by these adjusted viewshed areas. The correction factors were relatively low, compared to some other vantage point survey datasets that I have analysed. This was due to the use of 1 km viewsheds, which mean that the distance bands with very low flightline densities did not contribute to the calculations.

Table 3.1. Adjusted viewshed areas compared to the original viewshed areas, and the correction factors representing the increase in collision risk generated by these adjusted viewshed areas.

VP	Viewshed height (m)	Original viewshed area (ha)	Adjusted viewshed area (ha)	Correction factor
VP1	14	142	74	1.9
VP1	20	142	74	1.9
VP1	50	142	74	1.9
VP1	100	142	74	1.9
VP2	14	114	61	1.9
VP2	20	114	61	1.9
VP2	50	128	66	1.9
VP2	100	128	66	1.9

Spatial patterns in flight activity within viewsheds can also be caused by habitat and/or topographical variation: e.g., due to species showing differences in flight activity between forestry and open habitats, or species avoiding high ground when commuting across a site. In large wind farm projects, the distance effects can be averaged across multiple viewsheds, and any such habitat or topographical factors are likely to balance out. In this project, there were only two vantage points used for this project. However, the habitats and topography within the viewsheds did not show strong variation with distance from the vantage points. Therefore, potential distance and habitat effects are not likely to be significantly confounded in the distribution of the mapped flightlines.

3.1.2. Species-specific spatial structure

The stage 1 model assumes random distribution of flight activity across the wind farm site, or across portions of it. Therefore, in addition to considering the distance effects on detectability, it is also necessary to consider whether deviations from this assumption are likely to significantly bias the model. In large wind farm sites, species are likely to show significant deviations from this assumption.

The Moanmore Lower Wind Farm site is a small site and the two viewshed arcs show a high degree of overlap. The habitats and topography within the viewshed arcs do not show strong

spatial variation. Therefore, spatial structure is not likely to have a high influence on the flight activity patterns recorded in the vantage point surveys.

3.1. TEMPORAL PATTERNS OF FLIGHT ACTIVITY

The recording rate of flightline records during each of the seasons covered by the vantage point survey is shown in Table 3.2. There was a general increase in Buzzard records over the period covered by the survey, which may reflect the continued expansion of this species in Ireland.

The recording rate of flightline records recorded during the vantage point survey is shown in Table 3.3. There were high rates of Hen Harrier records in May and June. Lesser Black-backed Gulls and Herring Gulls were recorded more frequently in summer than during the winter

3.2. HEIGHT BAND DISTRIBUTION OF FLIGHT ACTIVITY

The height band distribution of flightline records is shown in Table 3.4 and the height band distribution of total flight activity (bird-secs) is shown in Table 3.5. The flight activity was concentrated in the 25-50 m height band. There were no flightline records from the > 180 m height band, while flight activity in the 100-180 m height band was low.

Table 3.2. Seasonal recording rate (records / 51 hours) of flightline records during the vantage point survey.

Species	2020/21 winter	2021 summer	2021/22 winter	2022 summer	2022/23 winter	2023 summer	2023/24 winter
Mallard	0	0	0	1.4	0.7	1.4	0.7
Cormorant	0	0	0	0	2.1	0	0
Little Egret	0	0	0	0	0.7	0	2.8
Grey Heron	1.4	1.4	1.4	2.8	4.2	2.8	2.8
Hen Harrier	1.4	2.8	4.2	2.8	4.2	9.2	2.1
Sparrowhawk	0	2.8	0	1.4	1.4	0	0.7
Buzzard	0	0	0	1.4	0.7	2.1	4.2
Golden Plover	0	0	0	0	0	0	0.7
Lapwing	0	0	0	0	0	0	1.4
Whimbrel	0	0	0	0	0	2.1	0
Curlew	0	0	0	1.4	0	0	0
Greenshank	0	0	0	0	0	0	1.4
Snipe	0	0	0	0	0.7	0.7	0.7
Black-headed Gull	0	0	0	0	0.7	0	0.7
Common Gull	0	0	0	0	1.4	0	0
Lesser Black-backed Gull	0	5.7	1.4	5.7	3.5	10.6	2.8
Herring Gull	0	11.3	2.8	11.3	2.1	9.9	7.8
Great Black-backed Gull	0	0	0	0	0	0.7	0.7
Kestrel	5.7	4.2	1.4	0	7.1	5	2.8
Merlin	0	0	0	0	2.1	0.7	2.1
Peregrine	0	0	0	2.8	0	0	0.7

This table includes all vantage point survey records, including flightlines outside viewsheds. The recording rate is shown as records / 51 hours because the mean survey duration per season was 51 hours.

Table 3.3. Monthly recording rate (records / 30 hours) of flightline records recorded during the vantage point survey.

Species	Jan	Feb	Mar	Apr	May	Jun	Jul	Aug	Sep	Oct	Nov	Dec
Mallard	0	0.8	0.8	1.2	0	2.9	0	0	0	0	0	0
Cormorant	0	1.7	0	0	0	0	0	0	0	0	0	0.8
Little Egret	0	0.8	0	0	0	0	0	0	0	0	1.7	1.7
Grey Heron	0.8	5.8	2.5	1.2	2.2	1.4	3.8	0	0	0	0.8	0
Hen Harrier	2.5	0.8	0.8	1.2	6.7	8.6	3.8	0	1.2	2.5	0.8	3.3
Sparrowhawk	0	0.8	0.8	1.2	1.1	0	1.2	0	0	0	0	0.8
Buzzard	0	0	0	0	0	1.4	1.2	0	2.5	2.5	2.5	0.8
Golden Plover	0	0.8	0	0	0	0	0	0	0	0	0	0
Lapwing	0	0	0	0	0	0	0	0	0	0	0	1.7
Whimbrel	0	0	0	0	2.2	0	0	0	1.2	0	0	0
Curlew	0	0	0	0	0	0	0	0	1.2	0	0	0
Greenshank	0.8	0	0	0	0	0	0	0	0	0	0	0.8
Snipe	0	0.8	0	0	0	0	0	0	1.2	0.8	0	0
Black-headed Gull	0	0	0	0	0	0	0	0	0	0	0.8	0.8
Common Gull	0	0	0	0	0	0	0	0	0	0	0	1.7
Lesser Black-backed Gull	0.8	0.8	2.5	5	3.3	7.1	5	1.2	7.5	0	1.7	2.5
Herring Gull	5.8	1.7	0.8	6.2	7.8	8.6	5	6.2	3.8	2.5	1.7	0.8
Great Black-backed Gull	0	0	0	1.2	0	0	0	0	0	0	0.8	0
Kestrel	2.5	1.7	1.7	1.2	1.1	1.4	3.8	1.2	3.8	2.5	5	2.5
Merlin	1.7	1.7	0	1.2	0	0	0	0	0	0	0	1.7
Peregrine	0	0	0	0	0	0	0	0	2.5	0.8	0	0

This table includes all vantage point survey records, including flightlines outside viewsheds. The recording rate is shown as records / 30 hours because the mean survey duration per month was 30 hours.

Table 3.4. Numbers of flightline records recorded in each height band.

Species	0-20 m	20-50 m	50-100 m	100-180 m
Mallard	3	2	0	0
Cormorant	1	2	0	0
Little Egret	3	1	1	0
Grey Heron	10	7	2	0
Hen Harrier	29	2	2	0
Sparrowhawk	5	1	0	0
Buzzard	3	4	2	1
Golden Plover	0	1	0	0
Lapwing	0	2	0	0
Whimbrel	1	1	1	0
Curlew	1	0	0	0
Greenshank	1	1	0	0
Snipe	0	1	2	0
Black-headed Gull	0	2	0	0
Common Gull	2	0	0	0
Lesser Black-backed Gull	8	15	7	1
Herring Gull	11	26	9	0
Great Black-backed Gull	0	0	2	0
Kestrel	9	18	7	0
Merlin	6	1	0	0
Peregrine	2	1	1	1
Total	**95**	**88**	**36**	**3**

This table includes all vantage point survey records, including flightlines outside viewsheds. There were no flightline records from the > 180 m height band.

Table 3.5. Total amount of flight activity (bird-secs) recorded in each height band.

Species	0-20 m	20-50 m	50-100 m	100-180 m
Mallard	64	40	0	0
Cormorant	12	82	0	0
Little Egret	17	20	130	0
Grey Heron	368	369	196	0
Hen Harrier	3644	100	190	0
Sparrowhawk	128	60	0	0
Buzzard	127	1320	630	240
Golden Plover	0	7	0	0
Lapwing	0	400	0	0
Whimbrel	30	252	16	0
Curlew	15	0	0	0
Greenshank	12	35	0	0
Snipe	0	1000	65	0
Black-headed Gull	0	187	0	0
Common Gull	66	0	0	0
Lesser Black-backed Gull	162	717	299	22
Herring Gull	526	1410	583	0
Great Black-backed Gull	0	0	160	0
Kestrel	2561	8734	2253	0
Merlin	122	16	0	0
Peregrine	20	5	25	100
Total	**7874**	**14754**	**4547**	**362**

This table includes the total durations of each flightline, rather than the adjusted durations used for the collision risk modelling (see Section 4.1.3, Re-calculation of flight durations).

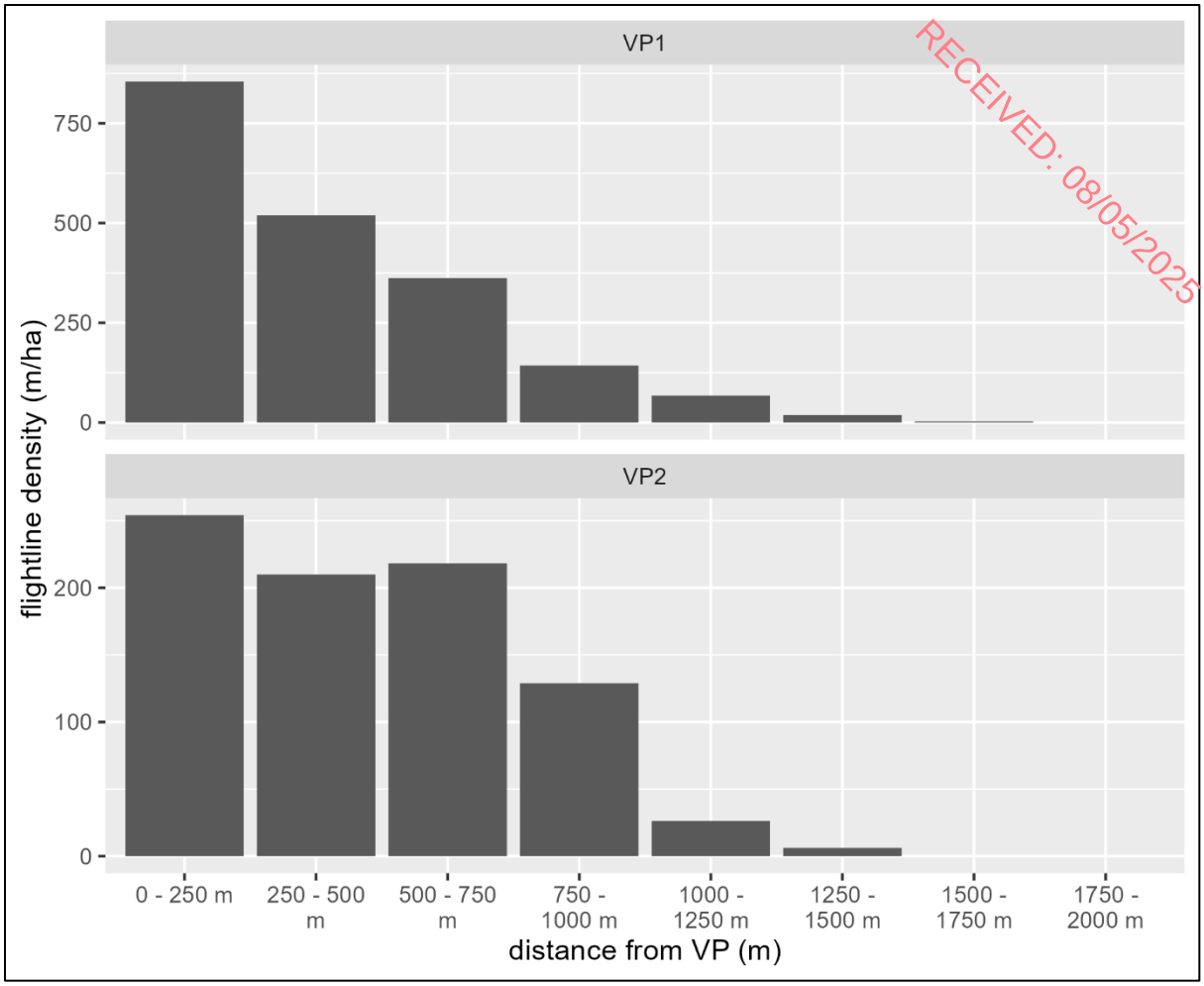

Figure 3.1. Flightline densities in 250 m distance bands from the vantage point locations.

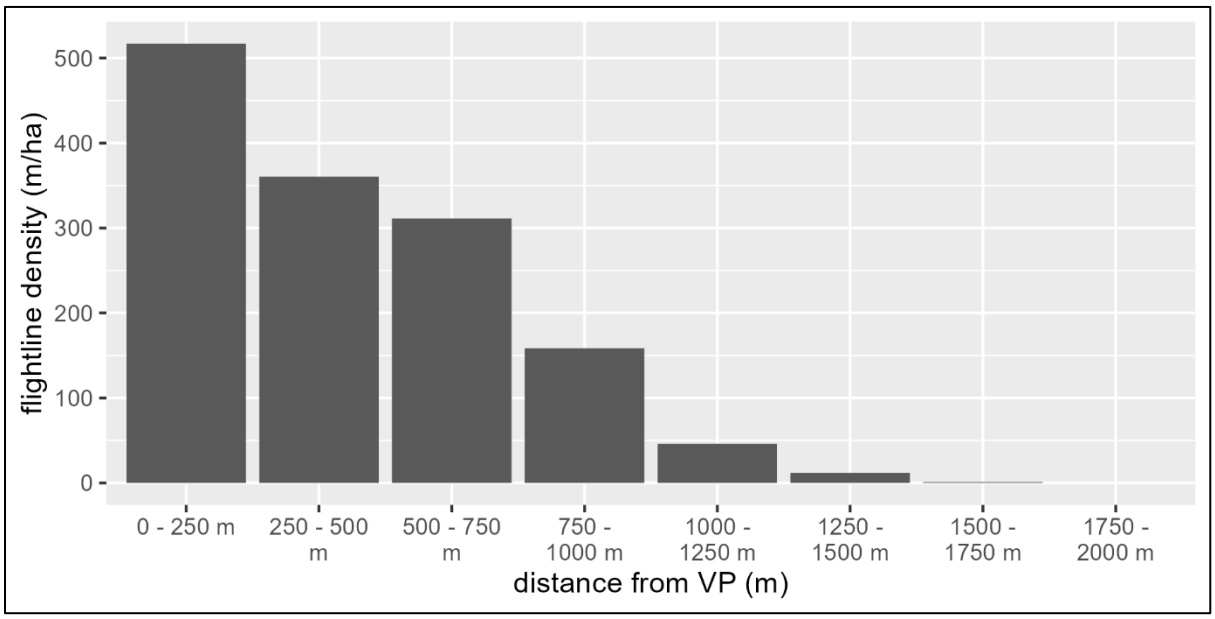

Figure 3.2. Weighted mean flightline densities in 250 m distance bands across the two vantage points.

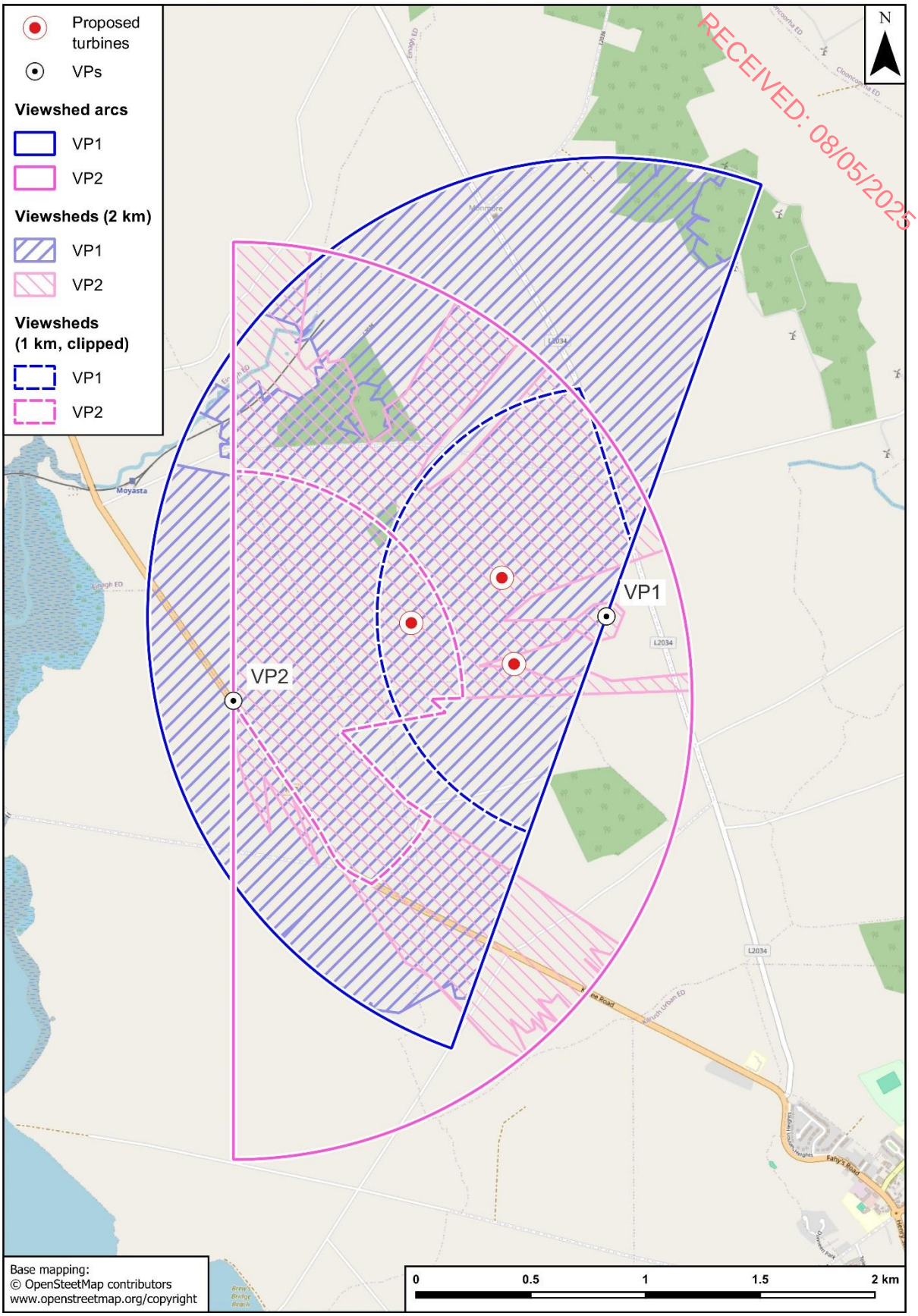

Map 3.1. Viewsheds mapped at 14 m above ground level.

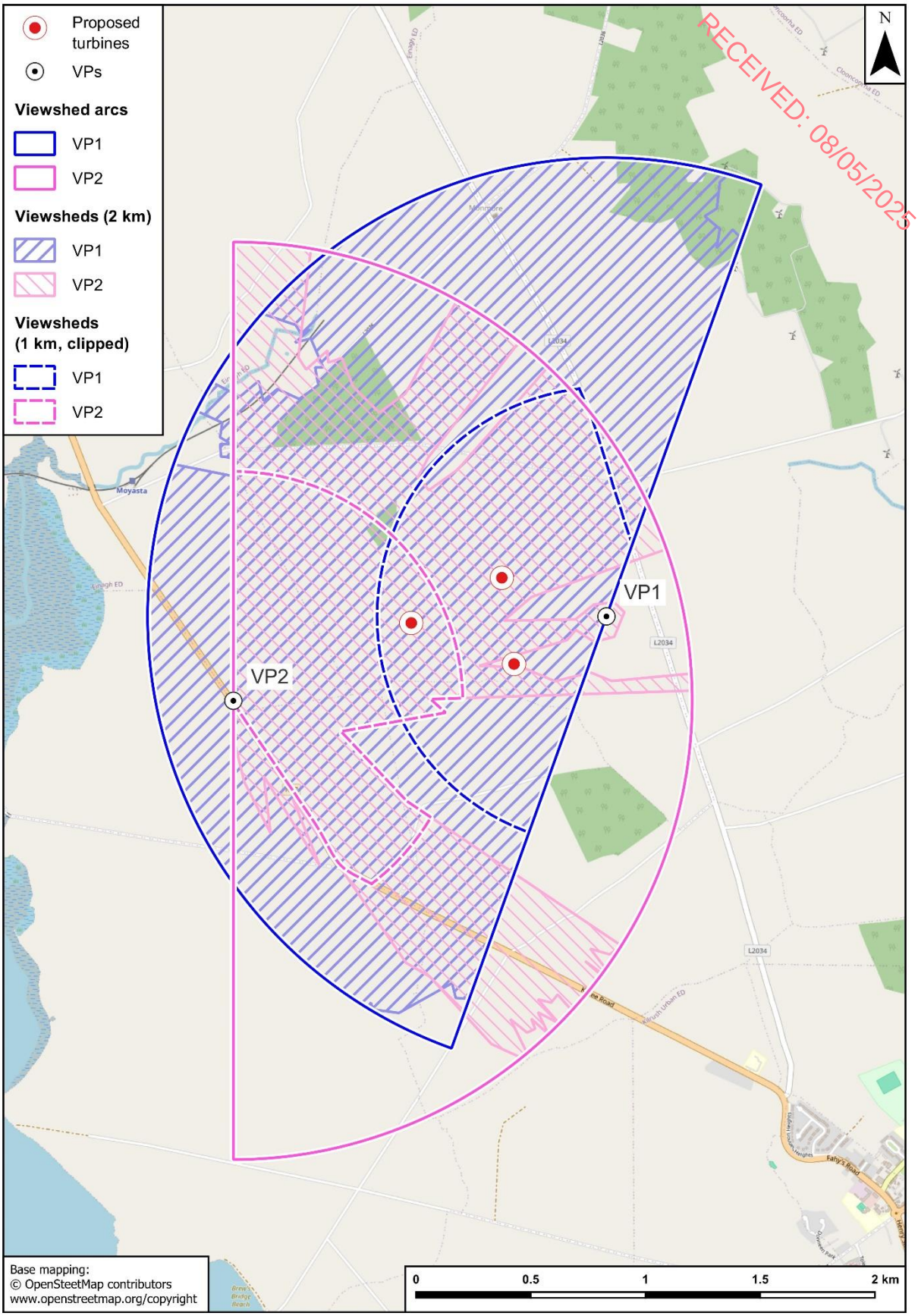

Map 3.2. Viewsheds mapped at 20 m above ground level.

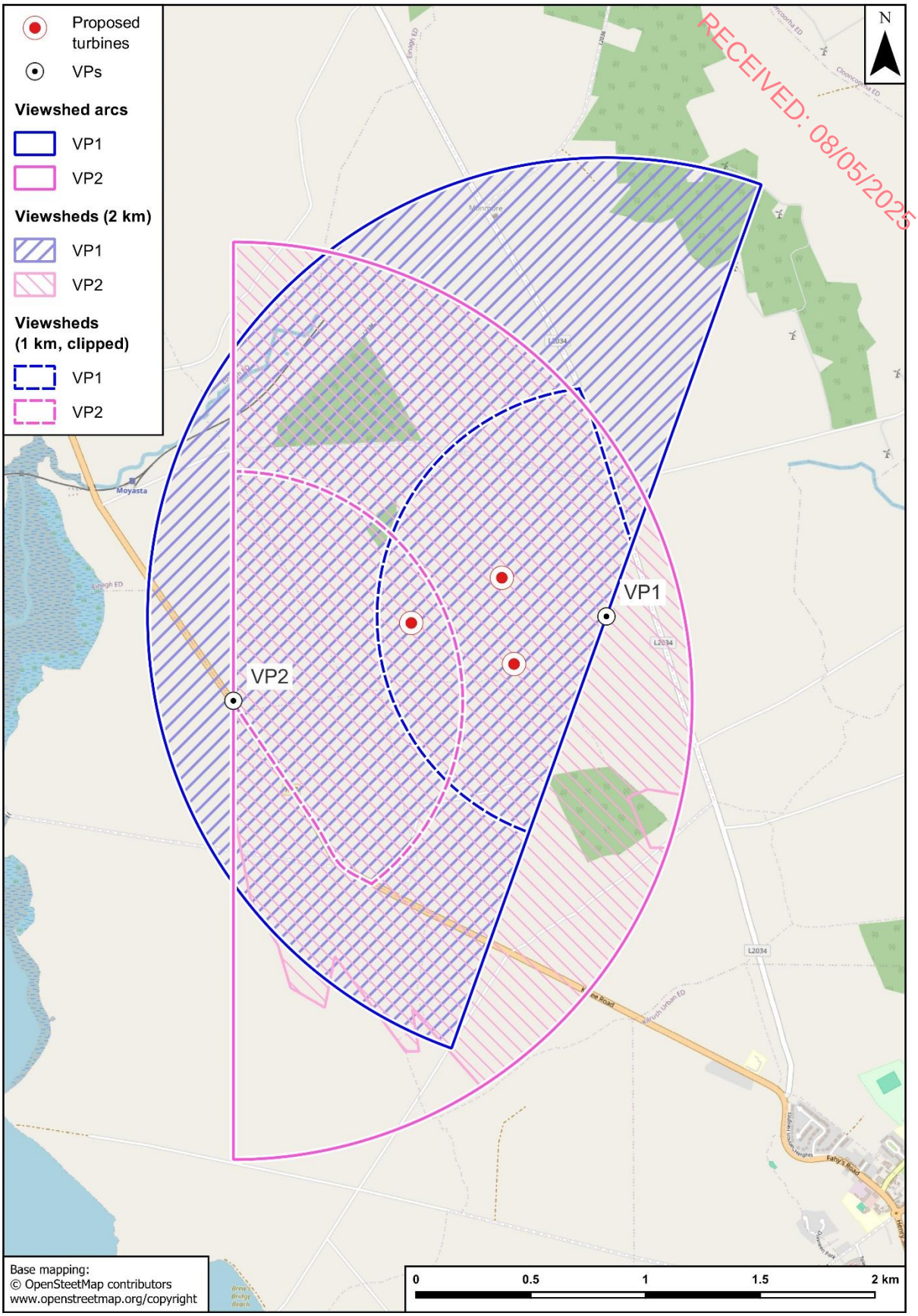

Map 3.3. Viewsheds mapped at 50 m above ground level.

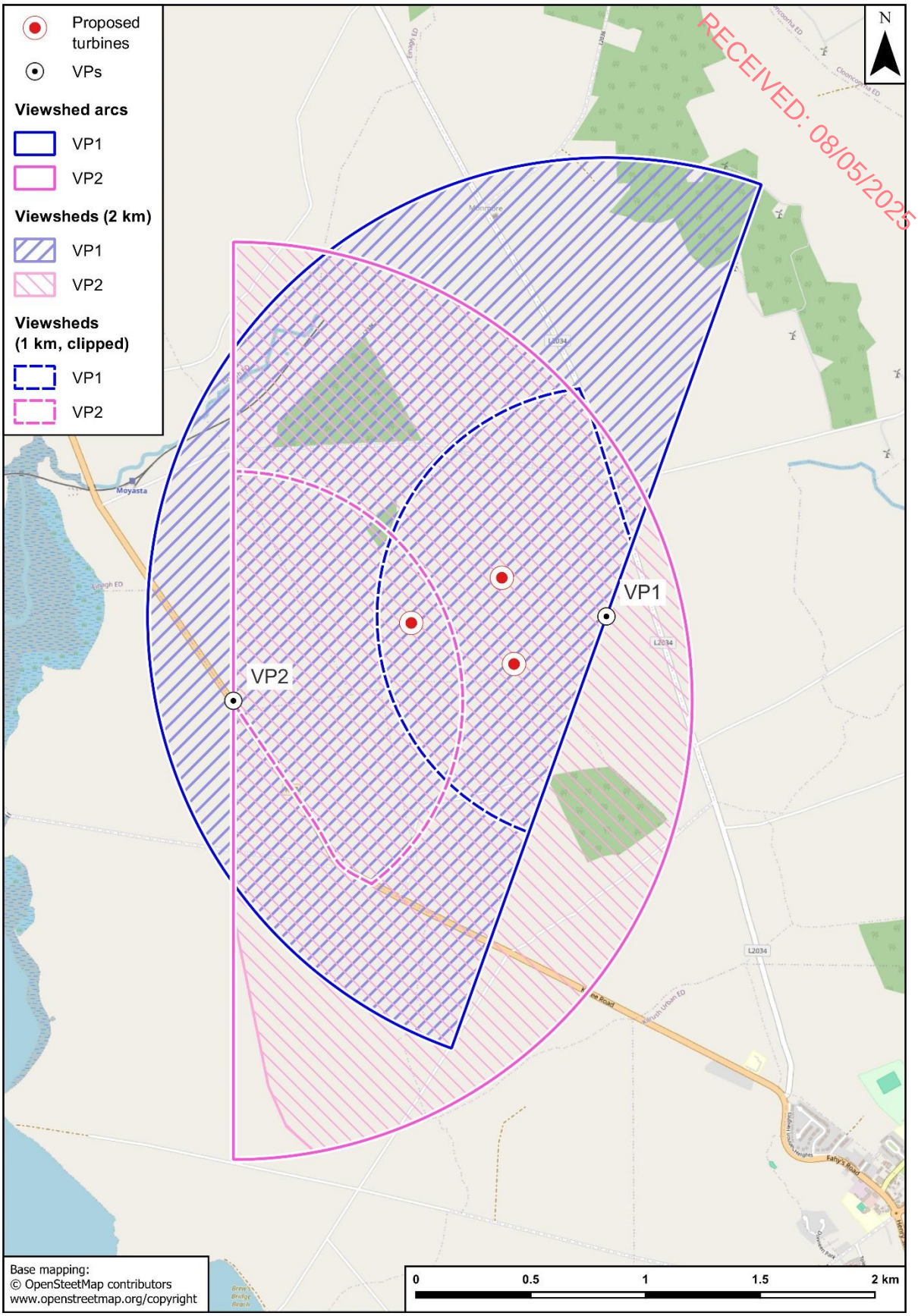

Map 3.4. Viewsheds mapped at 100 m above ground level.

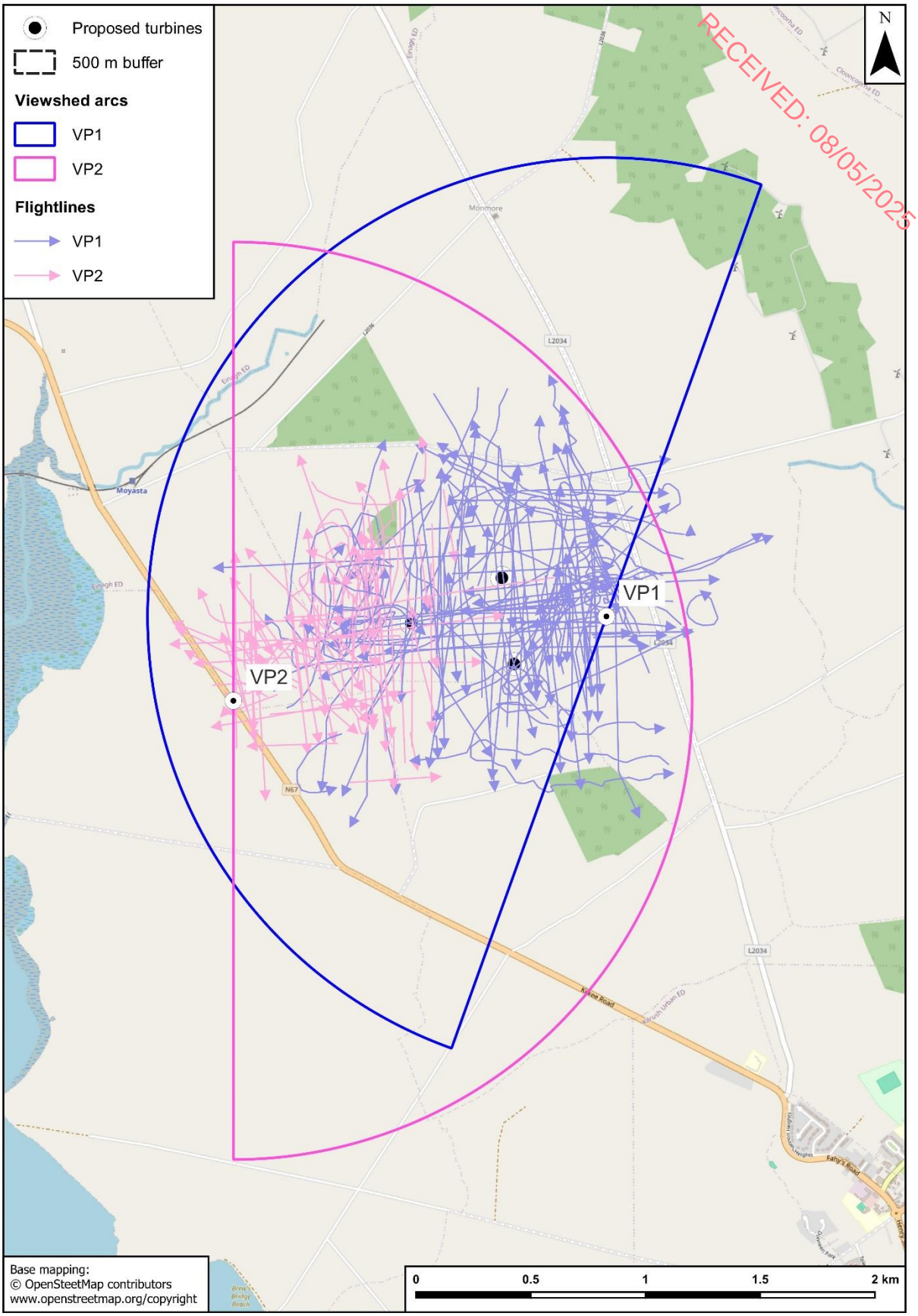

Map 3.5. Distribution of mapped flightlines from the vantage point survey in relation to the viewshed arcs.

4. COLLISION RISK MODEL STAGE 1: BIRD TRANSITS

4.1. METHODOLOGY

4.1.1. General approach

The stage 1 calculations use the vantage point survey data to calculate the predicted number of bird transits across the rotor swept volume. There are two methods described by SNH (2000) for carrying out stage 1 calculations: the "risk window" approach for when birds make regular flights through the flight risk area (e.g., geese commuting between roost sites and feeding areas); and the "bird occupancy" approach for when birds show variable patterns of flight activity within the flight risk area. I have used the "bird occupancy" approach, as this is generally the appropriate method for species that show variable patterns of flight activity, and the vantage point survey data and flightline mapping do not indicate regular flightlines through the wind farm site.

The sequential calculations that derive the predicted number of bird transits across the swept volume are shown in Table 4.1.

Table 4.1. Calculations of predicted number of bird transects across the rotor swept volume.

Step	Parameter	Calculation	Formula	Units	Details
1	t_1	bird-secs observed at potential collision height / total duration of VP watches	D_{bird}/VP_{eff}	birds	Mean number of birds observed flying at rotor height during the vantage point watches
2	n	t1 * total duration of season	$t_1 \times D_{season} \times 3600$	bird-secs	Predicted total number of birds observed flying at rotor height if the vantage point watches had covered the entire season
3	b	n × (volume swept by rotors / flight risk volume)	$n \times (A_{rotor} \times (L_{rotor}+L_{bird}))/(A_{vis} \times H_{rotor})$	bird-secs	Predicted bird occupancy of the swept volume across the entire season
4	$N_{transits}$	b / time taken for a bird to fly through rotors of one turbine	$b/((L_{rotor}+L_{bird})/v_{bird})$	bird transits	Predicted number of transits across the swept volume across the entire season

Note: The SNH (2000) calculation procedure include additional steps, which calculate flight activity within the "risk area", and then correct for the proportion of the risk area airspace occupied by the rotor swept volume of the turbines. However, these steps cancel out, so the calculation procedure shown in this table produces identical results.

The calculations in Table 4.1 simplify as Equation 3, which is shown below:

Equation 3: $N_{transits} = (D_{bird} \times D_{season} \times N_{turb} \times A_{rotor} \times v_{bird}) / (H_{rotor} \times VP_{eff} \times A_{vis})$

D_{bird} = bird-secs observed at potential collision height, D_{season} = total daylight hours across the season, N_{turb} = number of turbines, A_{rotor} = area of rotor discs, v_{bird} = bird flight speed, H_{rotor} = rotor diameter, VP_{eff} = total duration of vantage point watches, and A_{vis}= total area of viewshed.

Note that the rotor depth (L_{rotor}) and bird length (L_{bird}), which are included in the sequential calculations in Table 4.1, cancel out. While bird length is required for the collision probability calculations in stage 2, the rotor depth parameter (L_{rotor}) is not usually required for collision risk modelling.

4.1.2. Model types

The basic mathematical method for calculating predicted transits using the occupancy method (as described above) is explained by SNH (2000), and, in any case, can be easily derived from first principles. However, SNH (2000) does not provide guidance on how to incorporate data from multiple vantage points in calculations of predicted transits. The simplest method (the combined VPs method) combines the data from all the vantage points, using the sum of the flight activity across all the vantage points for the D_{bird} value, and the sum of the viewshed areas for the A_{vis} value. This method assumes that flight activity is randomly distributed throughout the combined viewsheds.

A slightly more sophisticated method is the VP averaging method. This involves calculating the flight activity density separately for each vantage point. The flight activity density is calculated using the same formula as Equation 1 but omitting N_{turb}. Then the mean flight activity density across all vantage points is used to calculate the overall number of transits predicted across the entire wind farm site. This is a variant of a method that is widely used (in Ireland) and has also been taught at courses on collision risk modelling run by the Chartered Institute of Ecology and Environmental Management[1]. This method also assumes that there is random distribution of flight activity across the wind farm site but treats each vantage point as a separate sample.

More sophisticated spatially-structured models can be developed by subdividing the overall wind farm site and modelling the transits separately for each section. However, as discussed above (Section 3.1.2), I did not consider that incorporating spatial structure was necessary for this collision risk model.

In this assessment I have modelled the predicted transits for all species using the VP averaging method.

I calculated the transits separately for each of the vantage point survey height bands included in the model. This allowed inclusion of larger viewshed areas for the higher height bands and also reduced the influence of inclusion of excess flight activity from the 0-20 m height band (see below).

4.1.3. Data preparation

Selection of species for the collision risk model

The vantage point survey dataset included flightline data for 21 raptor and waterbird species. All of these species were included in the collision risk model, apart from Snipe. The flight activity of Snipe is not effectively sampled by standard vantage point survey methods, due to its high level of crepuscular and nocturnal flight activity. Therefore, collision risk modelling based on the vantage point survey dataset would not produce meaningful results.

Height bands

The potential collision height zone for the turbine model that is proposed for this project occupies a height band of 14-150 m above ground level.

I used data from the following vantage point survey height bands: 0-20 m, 20-50 m, 50-100 m and 100-180 m.

The 0-20 m height band will have included a significant amount of flight activity below the potential collision height zone; in fact, the majority of flight activity in this height band may have occurred below the potential collision height zone. However, the calculation of transits separately for each height band reduced the influence of this excess flight activity.

The 100-180 m height band may have included flight activity above the potential collision height zone. However, the low level of flight activity in this height band means that the inclusion of excess flight activity in this height band will not have had much effect on the predicted collision risk.

For Hen Harrier, over 90% of the flight activity was in the 0-20 m height band and most of this flight activity was likely to have been below the potential collision height zone. There were eight Hen Harrier records where the estimated flight height was noted in the comments. Of these, seven were below the potential collision height zone (height ranges of 1-2 to 5-8 m) and one just reached the potential collision height zone (height range of 10-15 m). I excluded the seven records with heights below the potential collision height zone. The other 22 Hen Harrier records did not have any further details about the flight height in their comments.

[1] The method that is widely used calculates predicted transits per turbine separately for each vantage point and then uses the mean predicted transits/turbine across all vantage points to calculate the overall number of transits predicted across the entire wind farm site. This is equivalent to the method used in this report when all viewsheds contain turbines. However, the method used in this report can also include data from viewsheds that do not contain turbines.

Definition of seasonal periods

The seasonal periods that I used for each species included in the stage 1 model are shown in Table 4.2. These were based on the analyses of the monthly occurrence patterns (see Table 3.3) and general knowledge of the species ecology in Ireland.

I defined multiple seasonal periods for Hen Harrier, Whimbrel, Lesser Black-backed Gull and Herring Gull to reflect the potential occurrence of separate populations of these species at different times of the year. For Hen Harrier, the September – March period represents the non-breeding season, while the April – August period represents the breeding season. For Whimbrel, the April – May period represents the spring migration season and the August – October period represents the autumn migration season. For Lesser Black-backed Gull, the April – July period represents the breeding season, the September – October period represents the autumn migration season, and the November – March period represents the winter season. For Herring Gull, the April – August period represents the breeding season and the September – March period represents the non-breeding season.

For Golden Plover, Lapwing and Greenshank, I defined single seasonal periods to represent their likely occurrence patterns of non-breeding / wintering populations.

I used the suncalc package (Thieurmel and Elmarhraoui, 2022) in R 4.2.2 (R Core Team, 2022) to calculate the total daylight hours for the seasonal occurrence period of each species.

Table 4.2. Seasonal periods used for each species included in the stage 1 model.

Species	Seasonal period	Total daylight hours	Total survey hours / VP
Mallard	All year	4492	180
Cormorant	All year	4492	180
Little Egret	All year	4492	180
Grey Heron	All year	4492	180
Hen Harrier	Apr-Aug	2371	60
Hen Harrier	Sep-Mar	2120	120
Sparrowhawk	All year	4492	180
Buzzard	All year	4492	180
Golden Plover	Oct-Apr	2160	120
Lapwing	Oct-Feb	1372	90
Whimbrel	Apr-May	909	25.5
Whimbrel	Aug-Oct	1162	42
Curlew	All year	4492	180
Greenshank	Sep-Mar	2120	120
Black-headed Gull	All year	4492	180
Common Gull	All year	4492	180
Lesser Black-backed Gull	Apr-Jul	1917	48
Lesser Black-backed Gull	Aug-Oct	1162	42
Lesser Black-backed Gull	Nov-Mar	1412	90
Herring Gull	Apr-Aug	2371	60
Herring Gull	Sep-Mar	2120	120
Great Black-backed Gull	All year	4492	180
Kestrel	All year	4492	180
Merlin	Sep-Apr	2540	132
Peregrine	All year	4492	180

The total daylight hours are the D_{season} values used for the stage 1 model. The total survey hours / VP are the VP_{eff} values used for the stage 1 model.

Re-calculation of flight durations

As some mapped flightlines extended outside the viewshed boundaries, I clipped the mapped flightlines by the viewsheds, and recalculated the flight durations and bird-secs by multiplying their original values by (clipped flightline length) / (original flightline length). I carried out this analysis separately for the flightline durations in each height band, using the viewsheds derived for the relevant height band.

There were four records for which no flightline mapping was available. These records were included in the model without any adjustments to their flight durations.

Rotor area

I calculated bird transits separately for each height band included in the model. To carry out these separate calculations, it was necessary to subdivide the overall rotor area (A_{rotor}) into the portions that occurred in each height band. To calculate the rotor area in each height band, the angles subtended by segments representing the 0-20 m, 20-50 m, and 50-100 m height bands were calculated using the following equations:

Equation 4: $\theta_{0\text{-}20} = 2 \times \cos^{-1}((H_{hub} - 20) / R_{rotor})$

Equation 5: $\theta_{20\text{-}50} = 2 \times \cos^{-1}((H_{hub} - 50) / R_{rotor})$

Equation 6: $\theta_{50\text{-}100} = 2 \times \cos^{-1}((H_{hub} - 100) / R_{rotor})$

H_{hub} = hub height; R_{rotor} = rotor radius.

I then calculated the rotor areas using the following equations:

Equation 7: $A_{rotor(0\text{-}20)} = 0.5 \times (\theta_{0\text{-}20} - \sin(\theta_{0\text{-}20})) \times R_{rotor}^2$

Equation 8: $A_{rotor(20\text{-}50)} = 0.5 \times (\theta_{20\text{-}50} - \sin(\theta_{20\text{-}50})) \times R_{rotor}^2 - A_{rotor(0\text{-}20)}$

Equation 9: $A_{rotor(50\text{-}100)} = 0.5 \times (\theta_{50\text{-}100} - \sin(\theta_{50\text{-}100})) \times R_{rotor}^2 - A_{rotor(0\text{-}20)} - A_{rotor(20\text{-}50)}$

Equation 10: $A_{rotor(100\text{-}180)} = A_{rotor} - A_{rotor(0\text{-}20)} - A_{rotor(20\text{-}50)} - A_{rotor(50\text{-}100)}$

Similarly, the rotor height (H_{rotor}) values for each height band were adjusted to equal the height of the rotor segment in the height band.

These calculations produced rotor areas of 225 m^2 for the 0-20 m height band, 2,852 m^2 for the 20-50 m height band, 6,605 m^2 for the 50-100 m height band, and 4,844 m^2 for the 100-180 m height band. The rotor height values were 6 m for the 0-20 m height band, 30 m for the 20-50 m height band, 50 m for the 50-100 m height band, and 50 m for the 100-180 m height band.

4.1.4. Stage 1 model implementation

I carried out the stage 1 model calculations in R 4.3.2 (R Core Team, 2023). As discussed above, I used the VP averaging method, calculated the transits separately for each height band, and used the seasonal periods in Table 4.2 to calculate VP_{eff} and D_{season} values for each species.

I first calculated the flight activity density in each height band separately for each viewshed using the equation below, which is a modified version of Equation 1:

Equation 11: $(D_{bird} \times D_{season} \times A_{rotor} \times v_{bird}) / (H_{rotor} \times VP_{eff} \times A_{vis})$

D_{bird} = bird-secs observed at potential collision height, D_{season} = total daylight hours across the season, N_{turb} = number of turbines, A_{rotor} = area of rotor discs, v_{bird} = bird flight speed, H_{rotor} = rotor diameter, VP_{eff} = total duration of vantage point watches, and A_{vis}= total area of viewshed.

I then averaged the flight activity density in each height band across the two viewsheds, multiplied these averaged values by the number of turbines to obtain the predicted transits in each height band, and then summed the predicted transits across the height bands to obtain the overall number of predicted transits.

The flight activity (D_{bird}) values used in the model are shown in Table A1.1 in Appendix 1. The seasonal duration (D_{season}) values are shown in Table 4.2. The rotor area (A_{rotor}) values are presented in Section 4.1.3 (Rotor area). The bird flight speed (v_{bird}) values are included in Table 2.2. The H_{rotor} values are presented in Section 4.1.3 (Rotor area). The survey effort (VP_{eff}) values

are shown in Table 4.2. The viewshed area (A_{vis}) values are shown in Table 3.1. The number of turbines used for the collision risk model was four.

4.1.5. Stage 1 model results

The results of the stage 1 calculations are shown in Table 4.3. The species with the highest predicted transits per year were Kestrel, Buzzard and Herring Gull with 636, 164 and 110 transits / year, respectively. All the other species had predictions of less than 100 transits / year.

Table 4.3. Predicted transits per year.

Species	Season	Transits / year
Mallard	all year	5.9
Cormorant	all year	8.1
Little Egret	all year	8
Grey Heron	all year	28
Hen Harrier	Apr-Aug	34
Hen Harrier	Sep-Mar	31
Sparrowhawk	all year	3.8
Buzzard	all year	164
Golden Plover	Oct-Apr	0.27
Lapwing	Oct-Feb	11
Whimbrel	Apr-May	74
Whimbrel	Aug-Oct	1
Curlew	all year	0.33
Greenshank	Sep-Mar	1.2
Black-headed Gull	all year	3.7
Common Gull	all year	2.5
Lesser Black-backed Gull	Apr-Jul	58
Lesser Black-backed Gull	Aug-Oct	34
Lesser Black-backed Gull	Nov-Mar	7.8
Herring Gull	Apr-Aug	83
Herring Gull	Sep-Mar	27
Great Black-backed Gull	all year	20
Kestrel	all year	636
Merlin	Sep-Apr	1.3
Peregrine	all year	0.19

5. COLLISION RISK MODEL STAGE 2: COLLISION PROBABILITY

5.1. METHODOLOGY

Stage 2 of the collision risk model involves calculating the probability of a collision when a bird makes a transit of the rotor swept volume.

The Scottish Natural Heritage collision risk model (SNH, 2000; Band *et al.,* 2007; Band, 2012) calculates the probability, p (r, φ), of collision for a bird at radius r from the hub and at a position along the radius that is at angle φ from the vertical. This probability is then integrated over the entire rotor disc, assuming that the bird transit may be anywhere at random within the area of the disc. Separate calculations are made for flapping and gliding birds and for upwind and downwind transits. This method assumes that: birds are of a simple cruciform shape; they fly through turbines in straight lines with a perpendicular approach to the plane of the rotor; their flight is not affected by the slipstream of the turbine blade; and that the turbine blades have width and pitch angle, but no thickness.

The collision probability calculations for the original Scottish Natural Heritage collision risk model can be carried out using an Excel spreadsheet which is provided as an accompaniment to the SNH (2000) guidance. This spreadsheet was updated by Band (2012) by changing the details of the blade profile used in the model. The updated model is included in R code provided by Masden (2015).

I carried out all the collision probability calculations in R 4.2.2 (R Core Team, 2022), using an adapted version of the R code provided by Masden (2015). I audited this R code against the Band (2012) spreadsheet to confirm that it produced matching collision probability calculations.

One of the turbine parameters used to calculate collision probability is the mean pitch angle of the turbine blade. This parameter specifies the angle of the blade from the horizontal, so the collision probability will increase as the mean pitch angle increases. Data on mean pitch angle can be difficult to obtain so generic values are often used in collision risk models. These are often based on the statement by Band (2012) that a mean pitch angle of "25-30 degrees is reasonable for a typical large turbine". However, Band was referring to offshore wind farms where wind speeds are higher than at onshore wind farms, resulting in higher mean pitch angles. For this assessment, I applied a more realistic scenario from an onshore wind farm (Meenwaun, Co. Offaly). The pitch angle over a continuous 12-month period at this site was for approximately 90% of the time between -3° and 9° (MKOS, 2019). I used a pitch value of 6° for the collision probability calculations, as this was the pitch value within the -3° to 9° range that produced the highest collision probability values for most species in the sensitivity analyses (see Section 5.4.1).

The bird biometric and turbine parameter values used in the calculations of collision probability are shown in Table 2.1 and Table 2.2. The proportions of upwind and downwind flight were set as 0.5.

5.2. RESULTS

The collision probability predictions are shown in Table 5.1. There were very small differences between the collision probabilities for flapping and gliding flight, so I have used the mean values in this model. These varied from around a 1 in 21 chance of a collision on a single transit for Golden Plover to around a 1 in 12.5 chance for Grey Heron. Note that these probabilities do not take account of avoidance rates.

Table 5.1. Probability of a collision on a single transit of the rotor airspace.

Species	Flapping	Gliding	Mean
Mallard	0.055	0.053	0.054
Cormorant	0.069	0.067	0.068
Little Egret	0.067	0.066	0.067
Grey Heron	0.082	0.079	0.080
Hen Harrier	0.065	0.063	0.064
Sparrowhawk	0.053	0.052	0.052
Buzzard	0.063	0.060	0.062
Golden Plover	0.048	0.045	0.047
Lapwing	0.051	0.049	0.050
Whimbrel	0.052	0.050	0.051
Curlew	0.056	0.054	0.055
Greenshank	0.051	0.050	0.051
Black-headed Gull	0.055	0.053	0.054
Common Gull	0.056	0.053	0.055
Lesser Black-backed Gull	0.063	0.060	0.061
Herring Gull	0.064	0.061	0.063
Great Black-backed Gull	0.067	0.064	0.065
Kestrel	0.055	0.054	0.054
Merlin	0.052	0.051	0.051
Peregrine	0.057	0.055	0.056

5.3. INTERPRETATION OF COLLISION PROBABILITY VALUES

Collision probability values are often misinterpreted. The collision probabilities represent the probability of a collision on a single transit of the rotor airspace. While they contribute to the calculation of the predicted collision risk, they should not be interpreted as providing any information about the likely magnitude of the predicted collision risk. The predicted transits have a much larger influence of the predicted collision risk and a species with a relatively high collision probability may have a very low predicted collision risk if the number of predicted transits is low.

5.4. SENSITIVITY

5.4.1. Pitch angle

Modern wind turbines have variable pitch angles, so I carried out sensitivity analyses to investigate how collision probabilities varied with pitch angle. I calculated collision probability values for each 1° increment in pitch angle between -5° and 90°.

The relationships between collision probabilities and pitch angles are shown in Figure 5.1 for the species included in the collision risk model. The collision probability values showed little variation up to pitch values of around 10-20°, after which they increased sharply with increasing pitch. The rate of increase was broadly related to flight speed, with species with slower flight speeds showing steeper increases.

As discussed above, monitoring data indicates that pitch angles at onshore wind farms in Ireland rarely exceed 9°. In the pitch angle range from -5° to 9°, the maximum collision probability for all the species occurred at a pitch angle of around 0° (Figure 5.2). Therefore, I used a pitch angle of 0° for modelling the collision probability for all species included in the collision risk model.

5.5. ROTATION SPEED

The rotation speed has a strong influence on the collision probability values. However, the rotation speed value used in the collision probability calculations was simply the mid-point of the rotor speed range. In practice, rotation speeds will vary with wind speed. Therefore, I carried out sensitivity analyses to investigate how collision probabilities varied with rotation speeds across the range of operational rotation speeds.

The relationships between collision probabilities and rotation speeds are shown in Figure 5.3 for the species included in the collision risk model.

The effects of variation in rotation speed generally increased with body size, but species with slow flight speeds showed steeper increases relative to their body sizes. For small species like Golden Plover, the variation in rotation speed, within the operational speed ranges, had negligible effects on the collision probabilities. However, for large species like Cormorant and Grey Heron, there was a 2-3% variation in collision probabilities across the operational speed ranges. For these two species, this variation would result in an increase in the predicted collision risk of up to 1.5 times between the minimum and maximum rotation speeds.

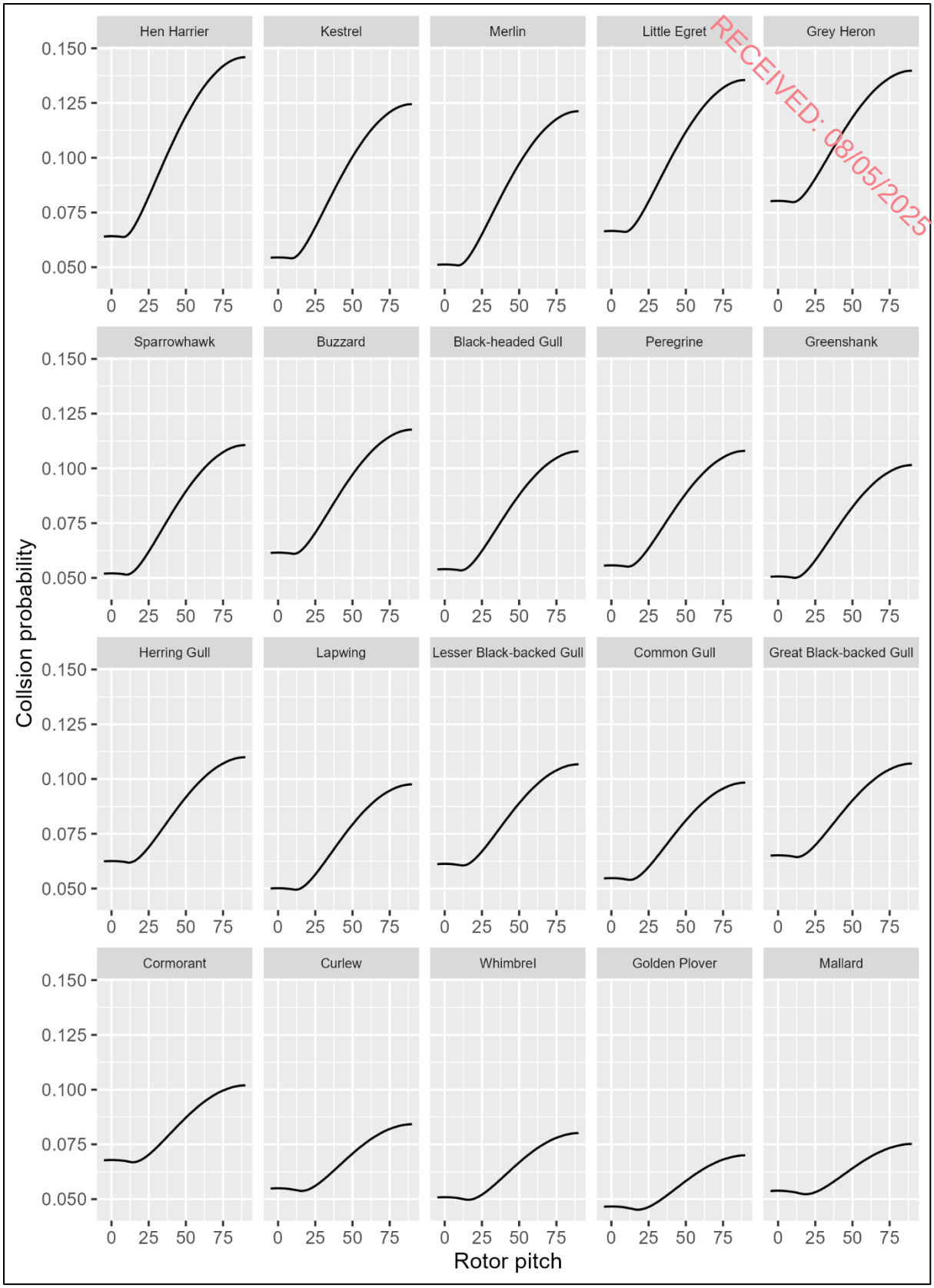

Figure 5.1. Relationship between collision probability and pitch angle, with species arranged in order of increasing flight speed.

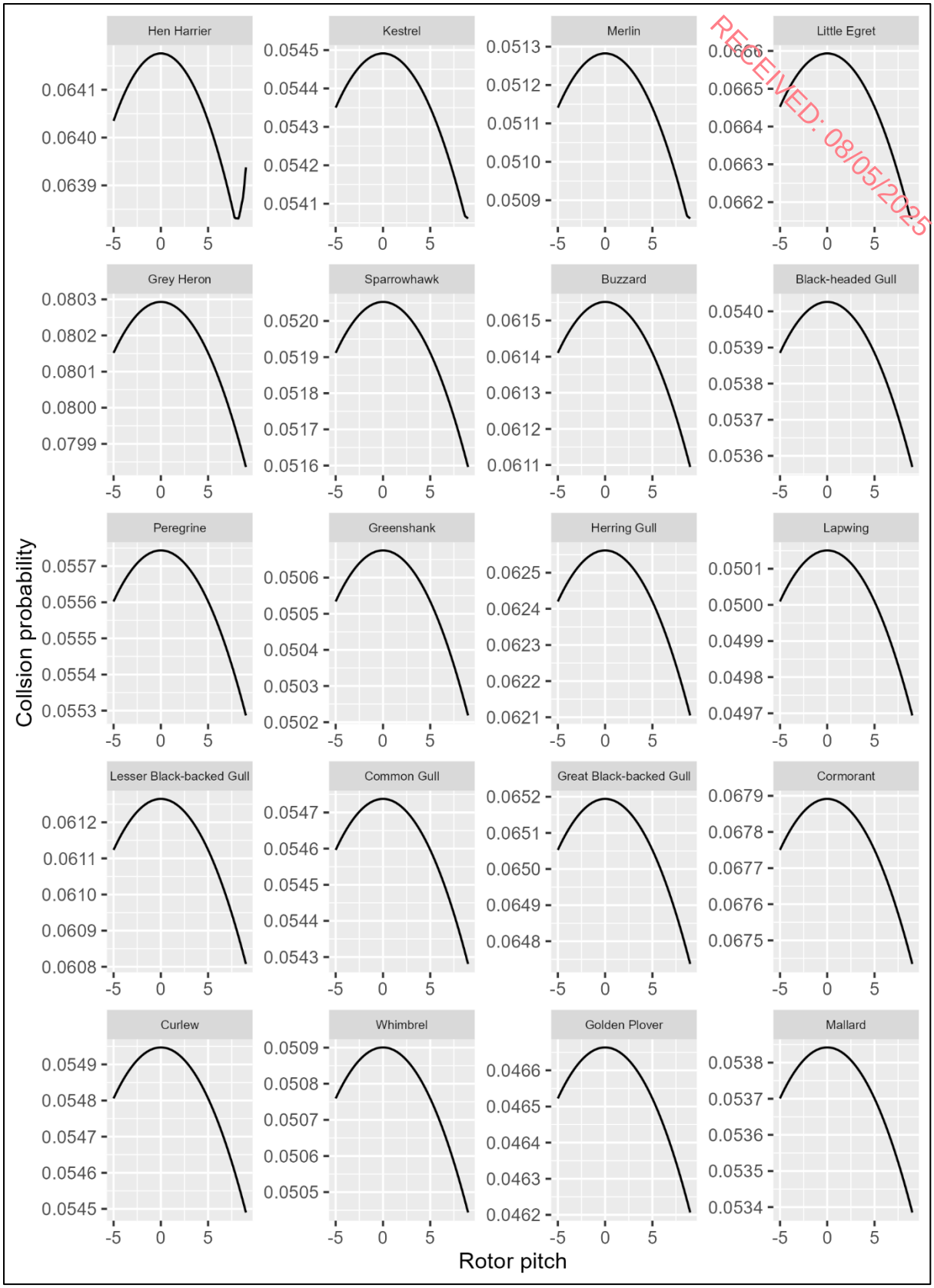

Figure 5.2. Maximum collision probabilities with pitch angle of between -5 and 9°, with species arranged in order of increasing flight speed.

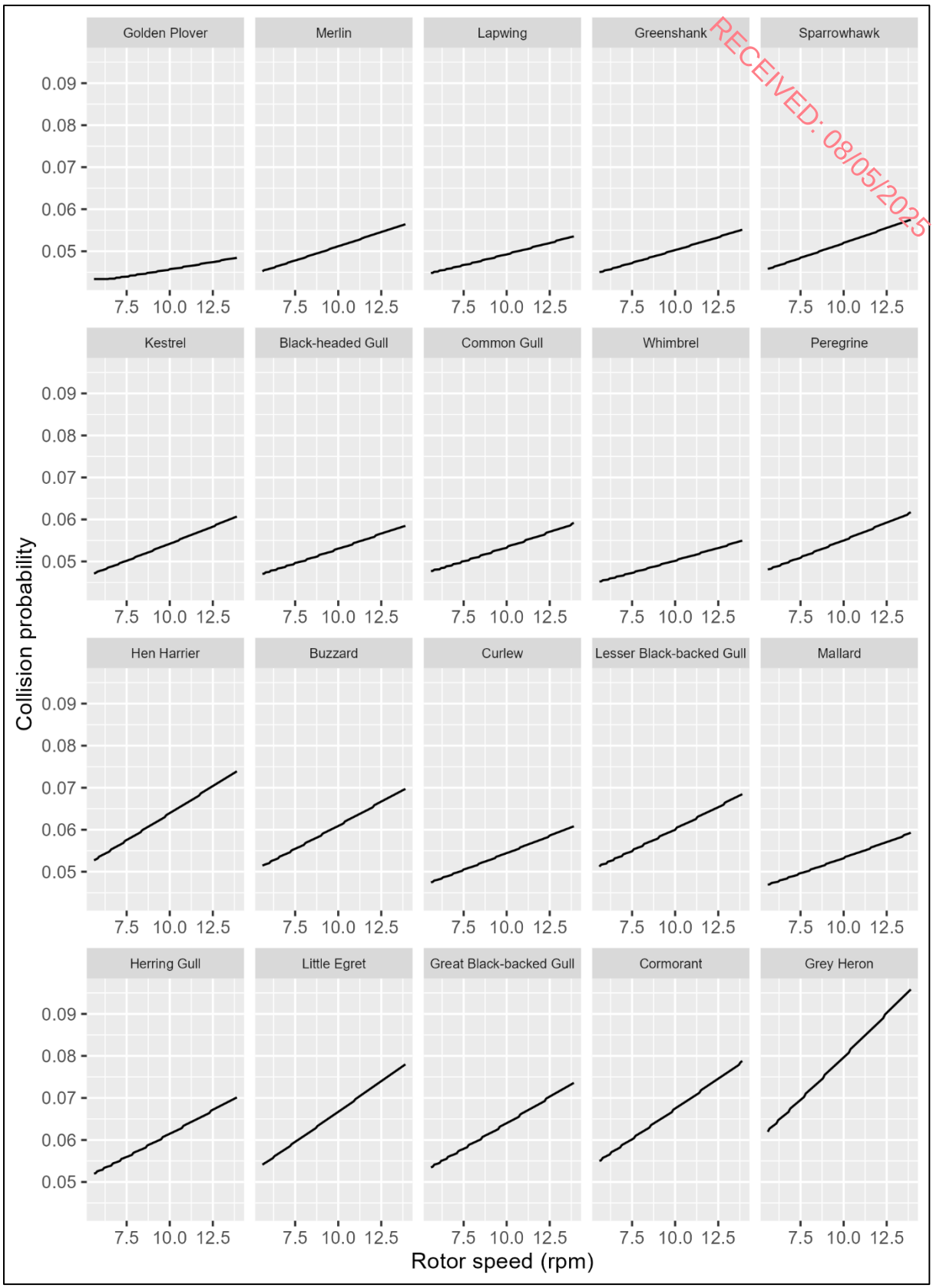

Figure 5.3. Relationship between collision probability and rotor speed, with species arranged in order of increasing body length.

6. COLLISION RISK MODEL STAGE 3: COLLISION PREDICTION

6.1.1. General

Stage 3 of the collision risk model uses the predicted transits from Stage 1 and the collision probabilities from Stage 2 to calculate the predicted collisions. However, three correction factors need to be considered: the avoidance rate; the degree of any nocturnal flight activity; and the proportion of time the wind farm is operational.

6.1.2. Correction factors

Avoidance rates

The avoidance rate reflects the fact that most potential collisions are avoided due to birds taking evasive action (SNH, 2010). This avoidance rate includes both behavioural avoidance (micro-avoidance) and behavioural displacement (macro-avoidance).

Behavioural avoidance is "action taken by a bird, when close to an operational wind farm, which prevents a collision". Behavioural displacement refers to the process by which a "bird may (possibly over time) change its home range, territory, or flight routes between roosting areas and feeding areas, so that its range use (or flight paths) no longer bring the bird into the vicinity of an operational wind farm".

Scottish Natural Heritage provides guidance on avoidance rates to use in collision risk assessments (SNH, 2010, 2018). For some species, including Hen Harrier and Kestrel, there is some evidence available that has been used to specify species-specific avoidance rates (SNH, 2018). In addition, a recent review for Scottish Natural Heritage has recommended the use of an avoidance rate of 0.995 for large gulls (including Lesser Black-backed Gull) at onshore wind farms (Furness, 2019). For the other species included in this collision risk model, the SNH guidance specifies a default avoidance rate of 98%.

The avoidance rates used in the stage 3 model are shown in Table 6.1.

Nocturnal flight activity

Another factor that needs to be considered is the degree of nocturnal flight activity that is likely to occur. The calculations of predicted transits are based on flight activity during daylight hours only. Therefore, if a species is likely to have a significant amount of nocturnal flight activity, a correction should be made to account for this nocturnal flight activity.

Correction factors for nocturnal flight activity were included for Mallard, Grey Heron, Golden Plover and Whimbrel. These correction factors were calculated using the following equation.

Equation 12: $ncf = 1 + nfr \times h_{night*} / h_{day*}$

nfr = nocturnal flight activity rate as a proportion of the diurnal flight activity rate; h_{night*} = mean night-time hours across seasonal period of occurrence; h_{day*} = mean day-time hours across seasonal period of occurrence.

The Whimbrel overflying the wind farm in spring are likely to be on direct migration, which is probably equally likely to occur by night as by day. So, the nocturnal flight activity rate for Whimbrel was set as 1.

The activity pattern of waders feeding on intertidal habitat follows the tidal cycle, rather than the diel cycle. Therefore, the nocturnal flight activity rate for Curlew and Greenshank was set as 1.

For Mallard, visual inspection of Figure 2 in Korner *et al.* (2016) suggests that nocturnal activity is around half that of diurnal activity, so the nocturnal flight activity rate was set as 0.5.

For Golden Plover, a figure of 25% of the day-time activity levels across the night-time hours is often used in collision risk modelling (e.g., MKOS, 2019), so the nocturnal flight activity rate was set as 0.25. The same value was used for Lapwing, due to the ecological similarity to Golden Plover of their habitat use in winter.

Flight activity patterns for Grey Heron from Vessem and Draulans (1987) indicate low levels of nocturnal flight activity, so the nocturnal flight activity rate was set at the same rate as Golden Plover. The same value was used for Little Egret.

The nocturnal flight activity rate for all other species was set as zero.

The nocturnal correction factors used in the stage 3 model are shown in Table 6.1.

Operational time

Wind turbines in operational wind farms will have periods when they are not turning due to maintenance or wind speeds. Therefore, the predicted collisions need to be corrected by the proportion of time the wind turbines will be operational. This value was set at 0.85 for all the species in the model, which is a widely used value for this parameter in collision risk modelling for onshore wind farms in Ireland.

6.1.3. Calculations

The collision risk was calculated using the following equation:

Equation 13: $cr = N_{transits} \times cp \times (1\text{-}ar) \times ncf \times op$

$N_{transits}$ = predicted transits per year; cp = collision probability (probability of a collision on a single transit); ar = avoidance rate; ncf = nocturnal correction factor; op = proportion of operational time.

6.2. COLLISION PREDICTIONS

The results of the stage 3 calculations are summarised in Table 6.1.

For Kestrel, the predicted collision risk would result in 44 collisions over the 30-year lifespan of the wind farm. The predicted collision risks would also result in at least one collision over the 30-year lifespan of the wind farm for Grey Heron, Hen Harrier (summed breeding and non-breeding season), Buzzard and Whimbrel.

The high value of predicted collision risk for Kestrel was due to a small number of records with very long flight durations. There was one record with a duration of 100 minutes, which contributed nearly half of the total amount of flight activity included in the model. There were also another three records with durations of 15-30 minutes each. Continuous flight activity for 100 minutes seems unlikely, while flight durations of 15-30 minutes are also on the high side. Therefore, it seems likely that there were some approximations in the recording of Kestrel flight activity that may have resulted in overestimation of the predicted collision risk.

The Hen Harrier predicted collision risk is probably also overestimated. Over 90% of the Hen Harrier flight activity was in the 0-20 m height band and it is likely that most of this flight activity was below the potential collision height zone (see Section 4.1.3, Height bands).

6.3. INTERPRETATION OF COLLISION RISK PREDICTIONS

6.3.1. General

A collision risk figure should be thought of as a probabilistic prediction rather than an absolute value and consideration should be given to the uncertainty around the prediction.

Some of the uncertainty relates to measurement error and imprecise specification of parameters, while sampling effects will also cause uncertainty.

6.3.2. Measurement error and imprecise specification of parameters

The effects of under-detection of distant flightlines on collision risk predictions have been discussed above (Section 3.1.1).

Other possible measurement errors in vantage point surveys include errors in allocation of flight activity to height bands, and errors in flightline mapping and/or determining when flightlines enter or leave viewsheds.

Table 6.1. Collision risk predictions.

Species	Season	Transits / year	Collision probability	Avoidance rate	Nocturnal correction factor	Collisions / year	Collisions / 30 years
Mallard	all year	5.9	0.054	0.98	1.48	0.0079	0.24
Cormorant	all year	8.1	0.068	0.98	1.00	0.0093	0.28
Little Egret	all year	8	0.067	0.98	1.24	0.011	0.34
Grey Heron	all year	28	0.080	0.98	1.24	0.048	1.0
Hen Harrier	Apr-Aug	34	0.064	0.99	1.00	0.019	0.56
Hen Harrier	Sep-Mar	31	0.064	0.99	1.00	0.017	0.51
Sparrowhawk	all year	3.8	0.052	0.98	1.00	0.0034	0.10
Buzzard	all year	164	0.062	0.98	1.00	0.17	5.0
Golden Plover	Oct-Apr	0.3	0.047	0.98	1.34	0.00029	0.0090
Lapwing	Oct-Feb	11	0.050	0.98	1.41	0.013	0.40
Whimbrel	Apr-May	74	0.051	0.98	1.61	0.10	3.0
Whimbrel	Aug-Oct	1	0.051	0.98	1.90	0.0017	0.050
Curlew	all year	0.3	0.055	0.98	1.95	6e-04	0.020
Greenshank	Sep-Mar	1.2	0.051	0.98	2.41	0.0025	0.080
Black-headed Gull	all year	3.7	0.054	0.992	1.00	0.0014	0.040
Common Gull	all year	2.5	0.055	0.992	1.00	0.00093	0.030
Lesser Black-backed Gull	Apr-Jul	58	0.061	0.995	1.00	0.015	0.45
Lesser Black-backed Gull	Aug-Oct	34	0.061	0.995	1.00	0.0087	0.26
Lesser Black-backed Gull	Nov-Mar	7.8	0.061	0.995	1.00	0.0020	0.060
Herring Gull	Apr-Aug	83	0.063	0.995	1.00	0.022	0.66
Herring Gull	Sep-Mar	27	0.063	0.995	1.00	0.0071	0.21
Great Black-backed Gull	all year	20	0.065	0.995	1.00	0.0055	0.17
Kestrel	all year	636	0.054	0.95	1.00	1.5	44
Merlin	Sep-Apr	1.3	0.051	0.98	1.00	0.0011	0.030
Peregrine	all year	0.2	0.056	0.98	1.00	0.00018	0.0050

The proportion of operational time was set as 0.85 for all species.

The use of the midpoint of the rotation speed range for the turbine rotation speed in the stage 2 model will affect the collision probability calculations, as the actual values of the turbine rotation speed during each potential collision event will vary. However, the sensitivity analyses (Section 5.5) suggest that this factor is not likely to have large effects on the predicted collision risk. For the species showing the largest variation, the difference in the collision probability values between the midpoint and the minimum and maximum rotation speeds was around 25% of the midpoint value. In practice, extreme values of rotation speed are likely to be relatively infrequent.

The stage 2 model also uses a mean pitch value, while the actual pitch values during each potential collision event will vary. However, the sensitivity analyses suggest that the effect of this factor is on the predicted collision risk will be negligible, within the range of pitch values that are considered typical for onshore wind farms in Ireland (Section 5.4.1).

6.3.3. Sampling effects

The standard vantage point survey effort following the Scottish Natural Heritage guidelines (SNH, 2017) only samples around 1.5-2% of the available daylight hours. The hours are usually distributed in a clustered way: e.g., the six hours per month at a vantage point are often done as back-to-back three-hour surveys for logistical reasons. As flight activity patterns for many species will not be evenly distributed, the low proportion of daylight hours sampled and the clustered distribution of the sampling, mean that the flight activity sampled may not be representative of the overall pattern of flight activity. This is a particular issue for species where a small number of flights could generate a large collision risk: e.g., a large Golden Plover flock circling around for an extended period of time.

There will also be year-to-year variation in flight activity patterns, due to a variety of factors such as variation in local population sizes, habitat changes, etc. As the lifespan of a wind farm is measured in decades, the survey period will only represent a snapshot of the potential variation in flight activity across the period when the potential collision risk will occur.

In the collision risk model for the Ummeras Wind Farm, I used bootstrapping procedures to resample the flight activity data and generate confidence intervals for the predicted collision risk for four species that had high levels of flight activity (Gittings, 2020). These collision risk models produced upper limits of the confidence intervals that were around 1.4 (Buzzard) to 2.4 (Golden Plover) times higher than the mean predicted collision risk. Conversely, the actual collision risk could be lower than the predicted collision risk.

6.3.4. Behavioural effects

The equation for calculating predicted transits (Equation 1) includes the mean bird flight speed as part of the numerator. However, for Kestrel, a significant proportion of their flight activity will typically involve hovering birds. The flight speed of a hovering Kestrel is close to zero (a small amount of drift in position will often occur during long bouts of hovering). Therefore, using the mean flight speed for Kestrel (10.1 m/sec; Alerstam *et al.*, 2007) in Equation 1 to predict transits of hovering Kestrel is clearly inappropriate and will result in highly inflated estimates.

In the collision risk model for the Castlebanny Wind Farm (Gittings, 2021), I used data collected during the vantage point survey on the duration of hovering flight, and the mean number of hovering positions per second, to calculate separate predicted transits for hovering Kestrels, with the standard stage 1 model only used for direct Kestrel flight activity. This resulted in a predicted collision risk that was less than half the value of the collision risk that would have been generated by using the standard stage 1 model for all Kestrel flight activity.

6.3.5. Allowing for uncertainty

The two main potential sources of uncertainty in collision risk modelling are the effects of under-detection of distant flightlines and sampling effects.

The use of 1 km viewsheds substantially reduced the effects of under-detection of distant flightlines. Correction factors were also included in the model to further address these effects., although there are some uncertainties associated with these correction factors, and they may underestimate the degree of correction required for small species like Kestrel.

To allow for the uncertainty associated with sampling effects, the predicted collision risks should be multiplied by factors of around 2-3 to represent a worst case scenario of the sampled flight activity being at the lower limit of the theoretical confidence intervals of the distribution of samples from the complete flight activity dataset. However, for Kestrel, the potential overestimation of the collision risk due to inclusion of hovering flight activity in the standard stage 1 model should also be considered.

7. CONCLUSIONS

The predicted collision risk for Kestrel would result in 44 collisions over the 30-year lifespan of the wind farm. However, there may have been some approximations in the recording of Kestrel flight activity that resulted in overestimation of the predicted collision risk.

The predicted collision risks would also result in at least one collision over the 30-year lifespan of the wind farm for Grey Heron, Hen Harrier, Buzzard and Whimbrel. However, the Hen Harrier collision risk was probably overestimated due to the mismatch between the height bands used for the vantage point survey and the ground clearance of the proposed turbine.

Sensitivity analyses indicated that variation in rotor speed within the rotor speed range, and variation in pitch values within the typical operational range for Irish onshore wind farms, would not significantly affect the collision risk predictions.

The use of 1 km viewsheds substantially reduces the potential effects of under-detection of distant flightlines on the collision risk predictions. Correction factors were also included in the model to further address these effects.

To allow for the uncertainty associated with sampling effects, the predicted collision risks should be multiplied by factors of around 2-3 to represent a worst case scenario of the sampled flight activity being at the lower limit of the theoretical confidence intervals of the distribution of samples from the complete flight activity dataset. However, for Kestrel, the potential overestimation of the collision risk due to inclusion of hovering flight activity in the standard stage 1 model should also be considered.

REFERENCES

Alerstam, T., Rosén, M., Bäckman, J., Ericson, P. G. P., & Hellgren, O. (2007). Flight speeds among bird species: Allometric and phylogenetic effects. PLoS Biol, 5(8), e197.

Band, B. (2012). Using a collision risk model to assess bird collision risks for offshore windfarms. Guidance document. SOSS Crown Estate.

Band, W., Madders, M., & Whitfield, D. P. (2007). Developing field and analytical methods to assess avian collision risk at wind farms. In Birds and wind farms: Risk assessment and mitigation (pp. 259-275). Quercus Editions.

Cramp, S., & Simmons, K. E. L. (2004). Birds of the Western Palearctic interactive (DVD-ROM). BirdGuides Ltd.

Furness, R. W. (2019). Avoidance rates of herring gull, great black-backed gull and common gull for use in the assessment of terrestrial wind farms in Scotland. Scottish Natural Heritage Research Report No. 1019. Scottish Natural Heritage.

Gittings, T. (2020). Castlebanny Wind Farm: Collision Risk Model. Unpublished report included as an appendix to the Castlebanny Wind Farm Environmental Impact Assessment Report.

Gittings, T. (2020). Ummeras Wind Farm: Collision Risk Model. Unpublished report included as an appendix to the Ummeras Wind Farm Environmental Impact Assessment Report.

Gittings, T. (2023). Distance effects on detection rates in wind farm vantage point surveys and their implications for collision risk modelling. Presentation at the 8th Irish Ornithological Research Conference, University College Cork, 11th March 2023.

Hijmans, R. (2023). terra: Spatial Data Analysis. R package version 1.7-55, <https://CRAN.R-project.org/package=terra>.

Masden, E. (2015). Developing an avian collision risk model to incorporate variability and uncertainty. Scottish Marine and Freshwater Science Vol 6 No 14. Scottish Government. https://doi.org/10.7489/1659-1

MKOS (2019). Cushaling Windfarm Site, Co. Offaly/Kildare: Collision Risk Assessment. Unpublished report included as an appendix to the Cushaling Windfarm Environmental Impact Assessment Report. McCarthy Keville O'Sullivan Ltd., Galway.

Pebesma, E. (2018). Simple Features for R: Standardized Support for Spatial Vector Data. The R Journal 10 (1), 439-446.

Pebesma, E., & Bivand, R. (2023). Spatial Data Science: With Applications in R. Chapman and Hall/CRC.

R Core Team (2023). R: A language and environment for statistical computing. R Foundation for Statistical Computing, Vienna, Austria. https://www.R-project.org/.

SNH (2000). Windfarms and birds: Calculating a theoretical collision risk assuming no avoiding action. Scottish Natural Heritage.

SNH (2010). Use of avoidance rates in the SNH wind farm collision risk model. Scottish Natural Heritage.

SNH (2017). Recommended bird survey methods to inform impact assessment of onshore wind farms. March 2017. Scottish Natural Heritage.

SNH (2018). Avoidance rates for the onshore SNH wind farm collision risk model. Scottish Natural Heritage.

Thieurmel B. & Elmarhraoui A. (2022). suncalc: Compute Sun Position, Sunlight Phases, Moon Position and Lunar Phase. R package version 0.5.1, <https://CRAN.R-project.org/package=suncalc>.

Appendix 1 Bird-secs data

Table A1.1. Bird-secs (D_{bird}) data used for the collision risk model.

Species	Season	VP	0-20 m	20-50 m	50-100 m	100-180 m
Mallard	All year	VP1	44	24	0	0
Mallard	All year	VP2	20	10	0	0
Cormorant	All year	VP1	8	0	0	0
Cormorant	All year	VP2	0	53	0	0
Little Egret	All year	VP1	4	0	130	0
Little Egret	All year	VP2	6	14	0	0
Grey Heron	All year	VP1	291	257	93	0
Grey Heron	All year	VP2	39	69	0	0
Hen Harrier	Apr-Aug	VP1	820	16	64	0
Hen Harrier	Apr-Aug	VP2	132	0	25	0
Hen Harrier	Sep-Mar	VP1	99	0	0	0
Hen Harrier	Sep-Mar	VP2	1186	49	0	0
Sparrowhawk	All year	VP1	117	41	0	0
Sparrowhawk	All year	VP2	10	0	0	0
Buzzard	All year	VP1	57	0	330	0
Buzzard	All year	VP2	70	1245	0	0
Golden Plover	Oct-Apr	VP1	0	6	0	0
Lapwing	Oct-Feb	VP1	0	389	0	0
Whimbrel	Apr-May	VP1	17	0	0	0
Whimbrel	Apr-May	VP2	0	252	0	0
Whimbrel	Aug-Oct	VP1	0	0	12	0
Curlew	All year	VP1	15	0	0	0
Greenshank	Sep-Mar	VP1	3	0	0	0
Greenshank	Sep-Mar	VP2	0	15	0	0
Black-headed Gull	All year	VP1	0	91	0	0
Common Gull	All year	VP1	1	0	0	0
Common Gull	All year	VP2	48	0	0	0
Lesser Black-backed Gull	Apr-Jul	VP1	59	382	30	15
Lesser Black-backed Gull	Nov-Mar	VP1	46	45	0	0
Lesser Black-backed Gull	Nov-Mar	VP2	15	5	55	0
Lesser Black-backed Gull	Apr-Jul	VP2	0	102	5	0
Lesser Black-backed Gull	Aug-Oct	VP2	0	122	70	0
Lesser Black-backed Gull	Aug-Oct	VP1	0	0	29	0
Herring Gull	Apr-Aug	VP1	195	477	475	0
Herring Gull	Apr-Aug	VP2	6	15	0	0
Herring Gull	Sep-Mar	VP1	81	552	32	0
Herring Gull	Sep-Mar	VP2	27	39	23	0
Great Black-backed Gull	All year	VP1	0	0	70	0

Species	Season	VP	0-20 m	20-50 m	50-100 m	100-180 m
Great Black-backed Gull	All year	VP2	0	0	90	0
Kestrel	All year	VP1	1541	7563	540	0
Kestrel	All year	VP2	1010	1032	1473	0
Merlin	Sep-Apr	VP1	24	9	0	0
Merlin	Sep-Apr	VP2	28	0	0	0
Peregrine	All year	VP1	12	0	0	0